Agricultural and Forest Meteorology 375 (2025) 110830

Contents lists available at ScienceDirect

Agricultural and Forest Meteorology

journal homepage: www.elsevier.com/locate/agrformet

Carbon emissions from forest harvest and fire offset approximately half of carbon sequestration of forestation in China during 1986-2020

Jin Mai [a,b,1], Yaoliang Chen [a,b,1,*], Qinghai Song [c], Zhiying Xu [d], Dengsheng Lu [a,b], Geping Luo [e]

[a] Key Laboratory for Humid Subtropical Eco-Geographical Processes of the Ministry of Education, Fujian Normal University, Fuzhou 350117, China
[b] School of Geographical Sciences, Fujian Normal University, Fuzhou 350117, China
[c] CAS Key Laboratory of Tropical Forest Ecology, Xishuangbanna Tropical Botanical Garden, Chinese Academy of Sciences, Menglun 666303, China
[d] Zhejiang Natural Resources Strategic Research Center, Hangzhou 310007, China
[e] State Key Laboratory of Desert and Oasis Ecology, Xinjiang Institute of Ecology and Geography, Chinese Academy of Sciences, Urumqi 830011, Xinjiang, China

ARTICLE INFO

Keywords:
Carbon budget
Forestation
Deforestation
Forest fire
Tree species
China

ABSTRACT

Forest activities and fire disturbance (FAFD) play an important role in the global carbon cycle. Although many studies have been explored to examine the individual effect of forestation, forest harvest, and forest fire on the carbon cycle in China, their combined impacts remain unclear. Moreover, rare research has been examined the impacts of these activities at the species level on the net carbon budget. By integrating remotely sensed, detailed tree species and statistical data into a spatialized modeling approach, we estimated the carbon budget from three major FAFD (i.e., forestation, forest harvest and forest fire) in China during 1986-2020. We found that FAFD overall showed net carbon sequestration of total -710.64±136.4 Tg C with sequestration of -1529.36 ± 202.59 Tg C from forestation and emission of 585.38 ± 29.91 Tg C from forest harvest and 233.34 ± 36.28 Tg C from fire. Spatially, the national average carbon sequestration density from FAFD was -172.95 Mg C km^{-2}, with notable regional variations. Carbon emissions from forest harvest and fire offset 53.52% (38.26% and 15.26%, respectively) of carbon sequestration from forestation. More than 90% of tree species exhibited net carbon sequestration from forestation and harvest. The national offset impact of forest harvest varied by tree species, ranging from 3.51% to 101.27%. Owing to high carbon emission from forest harvest, *Quercus* and *Eucalyptus* showed large offset effects over 97%. In contrast, *Pinus tabulaeformis* and *Larix* demonstrated small offset effects of only 3.51% and 10.23% due to high carbon sequestration. These findings highlight the importance of accounting for carbon emissions from deforestation and forest fire when aiming to maximize carbon sequestration through forestation.

1. Introduction

Forest activities and disturbance (FAFD) are fundamental in shaping forest structure and dynamics, significantly influencing the carbon sequestration capacity of forest ecosystems (Guimberteau et al., 2017; Kaimowitz, 2018; Kelly et al., 2020; Turner, 2010; Yang and Huang, 2021; Yu et al., 2022). Forestation contributed about 1.3 Pg C annually to the global carbon sink (Friedlingstein et al., 2023). Forest harvest as one of forest activities, acted as a major disturbance, representing the second-largest anthropogenic source of CO_2 emissions, after fossil fuel combustion (IPCC, 2019; Pan et al., 2024). Forest fire, another important disturbance, contributed approximately 2 Pg C per year in emissions, accounting for about 20% of anthropogenic carbon sources (van der Werf et al., 2017; Zheng et al., 2021). Estimating the carbon budget associated with FAFD and assessing their contribution at the national scale are critical for achieving China's carbon neutrality goals.

Four primary methodologies have been developed to estimate the carbon budget of FAFD. They include forest inventory method (Dixon et al., 1994; Fang et al., 2001; Pan et al., 2011; Piao et al., 2009), empirical statistical models (Fehrmann and Kleinn, 2006; Houghton and

* Corresponding author at: School of geographical sciences, Fujian Normal University.
E-mail addresses: 1319.sigma@gmail.com (J. Mai), chenyl@fjnu.edu.cn (Y. Chen), sqh@xtbg.ac.cn (Q. Song), xuzyhappy11@gmail.com (Z. Xu), ludengsheng@fjnu.edu.cn (D. Lu), luogp@ms.xjb.ac.cn (G. Luo).
[1] Jin Mai and Yaoliang Chen Contributed equally to this study.

https://doi.org/10.1016/j.agrformet.2025.110830
Received 26 January 2025; Received in revised form 7 August 2025; Accepted 31 August 2025
Available online 9 September 2025

Nassikas, 2017), process models (Piao et al., 2009; Piao et al., 2017; Sitch et al., 2008), and atmospheric inversions (Bousquet et al., 2000; Gurney et al., 2002; Wang et al., 2020). Many studies have applied these methods to estimate the carbon budget of China's FAFD (Pan et al., 2011; Piao et al., 2009; Chang et al., 2022; Tong et al., 2020; Yu et al., 2020, 2024). However, considerable discrepancies existed across estimates, even within the same approach. For instance, estimates based on forest inventory survey ranged from 137.3 to 201.1 Tg C yr^{-1} (Fang et al., 2007; Fang et al., 2018; Piao et al., 2009). The Chinese government's estimates, following IPCC National Greenhouse Gas Inventory Guidelines, spanned from 111.1 to 313.9 Tg C yr^{-1} (Department of Climate Change, Ministry of Ecology and Environment of China, 2018; National Development and Reform Commission of China, 2004, 2012, 2016, 2018a). Estimates based on process models ranged from 118 to 290 Tg C yr^{-1} (He et al., 2019; Jiang et al., 2016; Piao et al., 2009; Stephens et al., 2007; Tian et al., 2011), while estimates from atmospheric inversion varied from 280 to 450 Tg C yr^{-1} (Jiang et al., 2016; Jiang et al., 2013; Piao et al., 2009; Wang et al., 2020; Yang et al., 2017; Zhang et al., 2014), with Wang et al. (2020) estimating as high as 1.1 Pg C yr^{-1}. These discrepancies mainly stemmed from data limitations and the inherent limitations of each method (Piao et al., 2022). For example, inventory method provides direct measurements of vegetation carbon stocks with high accuracy, but it requires substantial labor and material resources, and suffers from long data-update cycles that cannot capture exactly annual carbon stock dynamics (Huang et al., 2023; Piao et al., 2022). Ecosystem process modeling method demands numerous input parameters (e.g., photosynthetic rate, respiration rate, soil carbon decomposition rate), and many of which rely on field measurements or empirical estimates, introducing significant uncertainties for simulating carbon budgets for diverse tree species at a national scale. Additionally, certain highly sensitive parameters (such as temperature sensitivity coefficients) may vary across different ecosystems or climatic conditions, leading to error propagation in model outputs (Piao et al., 2022). The atmospheric inversion method offers a distinct advantage of enabling real-time assessment of terrestrial carbon sink dynamics and their climate responses at global scales. However, the spatial resolution of net carbon flux estimates derived from this approach remains relatively coarse, limiting its capacity to accurately differentiate carbon fluxes among distinct ecosystem types and overcome constraints imposed by the limited number and uneven distribution of monitoring stations (Peylin et al., 2013; Piao et al., 2022). Although empirical models lack mechanism and cannot adequately represent plant biological characteristics, their simple data requirements, operational convenience, and incorporation of detailed regional vegetation parameters allow them to produce reasonably reliable results (Chen et al., 2016; Houghton et al., 2012).

Although the empirical-based models lack biophysical processes, their estimates can still be highly reliable when detailed data and localized parameters are used (Houghton and Nassikas, 2017). The Bookkeeping model is a notable example of such an empirical model, and has been widely used to estimate the carbon budget globally (Friedlingstein et al., 2023; Houghton, 2005; Houghton et al., 1983) and regionally like China (Houghton and Hackler, 2003), Europe (Olofsson et al., 2009; Kuemmerle et al., 2011), and the United States (Houghton, et al., 1999). Several studies have also assessed the carbon budget of FAFD at the provincial scale in China (Chen et al., 2016; Wang et al., 2022), though a comprehensive assessment at national scale is still lacking. In addition, existing studies by Bookkeeping model on FAFD typically used coarse plantation functional types, without detailing tree species or specific parameters (e.g., vegetation carbon density). The usage of coarse vegetation types introduced significant uncertainty in the final estimates. Moreover, many studies assumed linear vegetation growth, which overlooked the natural S-shaped growth patterns of trees (Cheng et al., 2023; Xu et al., 2017; Xu and Li, 2010). Another challenge is the spatialization of modeling results. Since FAFD statistics are typically aggregated at the provincial or national level, pixel-scale modeling is challenging due to the lack of specific location data. Consequently, carbon budget results lack spatial details. However, the availability of remote sensing products, such as land cover change data (Xia et al., 2023; Yang and Huang, 2021; Zhang et al., 2024), forest fire distribution data (Loboda, 2018; Randerson et al., 2018), and forest disturbance data (Goward, 2016; Hansen et al., 2013; Liu et al., 2023), offers a solution to generate spatial distribution of carbon budget. By integrating these remote sensing products with forest activity statistics, a spatially explicit Bookkeeping model framework could be developed, enabling the spatial modeling of carbon budget for FAFD.

In summary, current research on carbon budget estimation for FAFD using empirical models faces challenges in parameter refinement, localization at the tree species level with appropriate growth curves, and spatialization at the pixel scale. This study aims to develop a spatially explicit, tree species–localized Bookkeeping model by integrating FAFD statistics (i.e., forestation area, harvested wood product volume, and fire-affected area), land cover change data, remote sensing products of forest fire and disturbance, detailed tree species data, and S-shaped growth curves. This framework will estimate the national carbon budget for FAFD in China from 1986 to 2020. The specific objectives are: (1) to identify the spatial patterns of three FAFD types: forestation, forest harvest, and forest fire; (2) to spatially simulate carbon budget of each FAFD with species-specific parameters; (3) to investigate carbon budget from the three FAFD types across different regions, periods, tree species in China; and (4) to assess the offset effect of carbon emission from forest harvest and fire on carbon sequestration from forestation.

2. Data and methods

2.1. Data collection

Fig. 1 illustrates the study's four main stages: data collection, data preprocessing, carbon budget modeling, and result analysis. The datasets used in this study include statistical data of forestation area, harvested wood product volumes, forest fire area, and tree species information at province level, model parameters from literature, remote sensing products of land use/cover, fire distribution and forest disturbances. Details can be found in Table 1 and supplementary materials.

2.2. Methods

2.2.1. Definition of different forestation and forest harvest types

In this study, forestation was divided into afforestation, reforestation after harvest (RAH), and reforestation after fire (RAF). Afforestation refers to the planting of forests on land that was not previously forested, while RAH refers to replanting after logging or clear-cutting, and RAF refers to reforestation on land affected by forest fire. Forest harvest was divided into two types: Harvest for reforestation (HFRFT) and Harvest for other land use (HFOLU). Note that HFRFT is RAH.

2.2.2. Data processing

(1) Carbon density

The collected carbon density of each tree species and forest type was checked for each province. For provinces lacking specific data, a simple gap-filling method was applied: missing values for carbon density were estimated using the mean values from other provinces within the same sub-climate zone. The averaged provincial carbon density of each tree species was used in estimating the carbon budget for forestation and forest harvest, while that of each forest type was used for carbon budget calculations of forest fire. The average vegetation carbon densities were used for forestation carbon budget estimates through the piecewise linear method. The specific vegetation carbon density of each major tree species in each province can be found in the Excel file named 'Parameters of local special Bookkeeping model.xlsx' in supplementary materials.

(2) The area and volume allocation process of the three types of

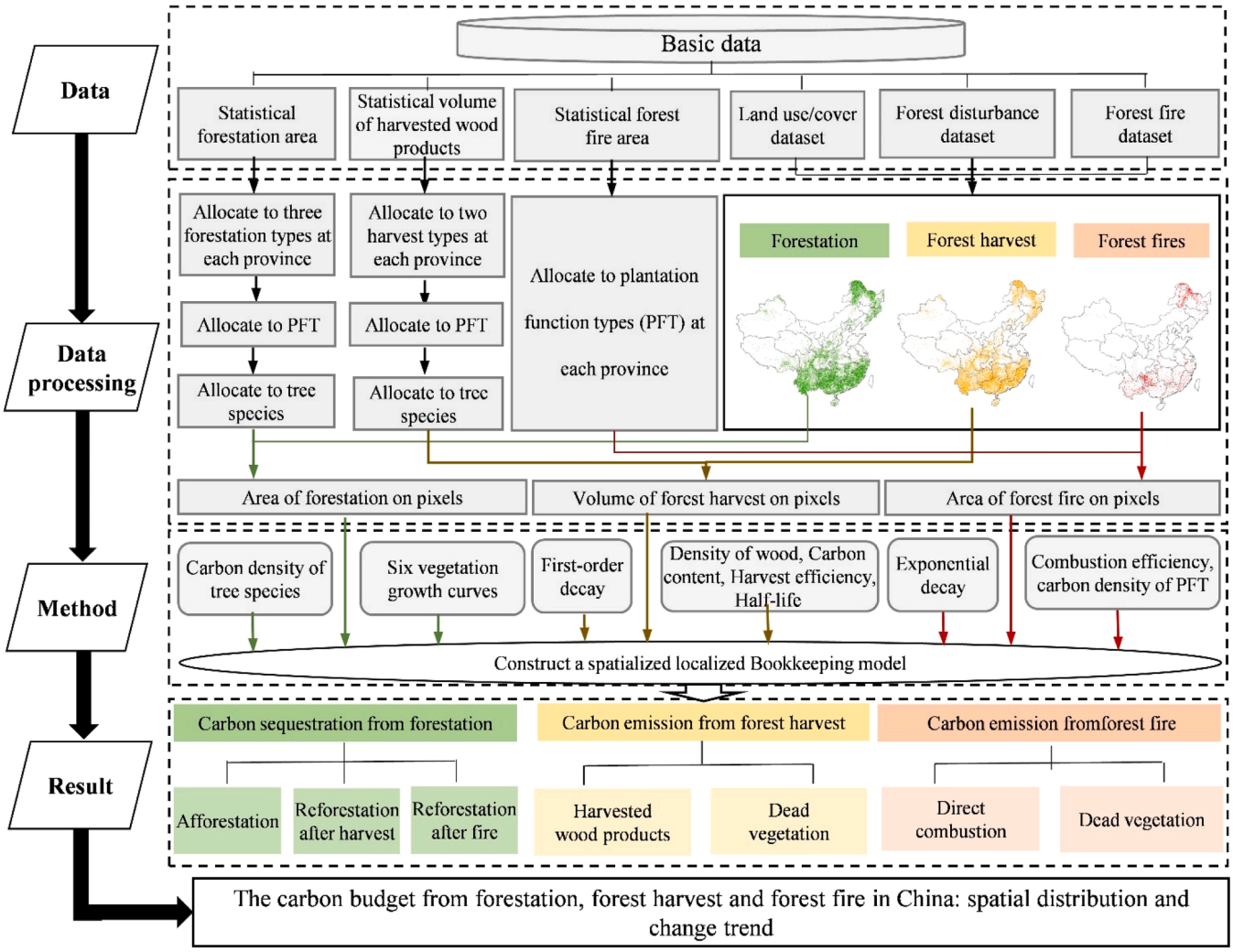

Fig. 1. Framework of this study.

FAFDs

We followed a five-step approach to allocate area or volume:

1) First, identifying the spatial locations of forestation, forest harvest, and forest fire by using remote-sensing datasets (Fig. 2a).
2) Second, determining the proportions of each forest type for each FAFD (Fig. 2b).
3) Third, allocating the statistical areas or volumes according to the aforementioned proportions of different forest types or activity-methods for each FAFD (Fig. 2b).
4) Fourth, distributing these allocated areas or volumes among the corresponding pixels of forest types and activity-methods at each FAFD (Fig. 2b).
5) Finally, allocating the area and volume allocated to each pixel among specific tree species, with the ratios obtained from the literature. It should be noted that forest fire was only specified to the forest - type level, so this last step does not apply to forest fire.

(a) Forest fire

Determining the Final Forest Fire Distribution for Each Year: Since the original spatial data for forest fire did not fully align with the forest extent in the land use/land cover dataset (due to differences in data sources), non-forested areas were removed from the forest fire dataset to ensure spatial consistency (Fig. 2a). This adjustment provided a more accurate spatial distribution of forest fire for this study. The resulting forest fire locations were then classified into five forest types based on the land use/land cover dataset: evergreen broadleaved forest, deciduous broadleaved forest, evergreen needle-leaved forest, deciduous needle-leaved forest, and mixed leaf forest (Fig. 2b).

Allocating Forest Fire Statistical Area to Each Pixel by Year: The provincial forest fire statistical area was proportionally distributed across pixels representing the five forest types. Allocation was based on each forest type's proportion, calculated by dividing the pixel count of each type by the total number of forest pixels within the province (Fig. 2b) (The detail of proportion for five vegetation types can be seen in the Excel file named 'Proportion of plantation function types.xlsx' in supplementary materials (https://data.mendeley.com/datasets/5kp76xww4r/3)). This ensured an accurate spatial representation of forest fire areas across different forest types annually.

(b) Forestation

Determining the Distribution of Three Forestation Types Annually: The distribution of afforestation was mapped through land cover change analysis conducted at two-year intervals. For reforestation after fire (RAF), distribution matched the locations of prior forest fire events, as RAF typically occurs in these fire-affected areas. Reforestation after harvest (RAH) was mapped by excluding overlaps with the newly identified forest fire distribution, afforestation area, and areas of harvest for other land use (HFOLU) from forest disturbance distribution (Fig. 2a). Once the three forestation types were allocated, each forestation pixel was classified into one of five forest types based on the land

Table 1
Data used in this study.

Data type	Category	Scale	Description	Source
Statistical data	Forestation area and forest fire area	1986-2020, Provincial scale	Area of protection, timber, economic, and fuel plantation from *China Forestry and Grassland Statistical Yearbook*; adjusted to 92% survival rate.	*China Forestry Statistical Yearbook* (http://202.99.63.178/c/www/tjnj.jhtml), *National Bureau of Statistics of China* (https://www.stats.gov.cn/).
	Harvested wood products (HWP) volume	1986-2020, Provincial scale	Volumes of fuelwood, paper wood, timber, and man-made wood from *China Forestry and Grassland Statistical Yearbook*.	
	Forest fire area	1986-2020, Provincial scale	1986–2017: *China Forestry and Grassland Statistical* Yearbook; 2018–2020: *National Bureau of Statistics of China.*	
Literature data	Tree species	Provincial scale	Provincial-level tree species for forestation/harvest.	*Forestry Professional Knowledge Service System* (http://lygc.lknet.ac.cn), CNKI (https://www.cnki.net), Web of science (https://webofscience.clarivate.cn/wos/alldb/basic-search)
	Classification of Age Classes and Age Groups	Regional scale	Age classifications from Forestry Industry Standards of China (National Forestry and Grassland Administration, 2018).	National Forestry and Grassland Administration (https://www.forestry.gov.cn/)
	Parameters of model	Provincial scale, Regional scale	Growth curve (a, b, c) of forestation, carbon density for tree species, harvest and fire model parameters from literature.	See the Excel file named 'Parameters of local special Bookkeeping model.xlsx' in supplementary materials (https://data.mendeley.com/datasets/5kp76xww4r/3) for details
Remote sensing data	Land use/cover dataset	1985-2020, 30 m × 30m	Global Land-cover Dynamic Monitoring Product with Fine Classification System with annual updates since 2000; accuracy: 80.88% (basic classification system), 73.24% (level-1 validation).	Zhang et al. (2024)
	Forest fire dataset	1985-2020, 30 m × 30m	Global Annual Burned Area Map with annual updates since 2000; user accuracy: 86.93%, producer accuracy: 69.97%.	Long et al. (2019)
	Forest disturbance dataset	1986-2020, 30 m × 30m	Annual updates; accuracy: 76% (forest fire), 96% (forest management)	Liu et al. (2023)

use/land cover dataset.

Allocation of Forestation Statistical Area to Each Pixel Annually: The area for each forestation type (afforestation, RAF, and RAH) was distributed proportionally based on the provincial forestation statistics. First, the area proportions of these three types were calculated by dividing the pixel count of each type by the total number of forestation pixels. Then, the actual forestation area assigned to each pixel was determined by dividing the statistical area of each forestation type by its corresponding pixel count, ensuring an accurate spatial allocation of forestation area at the pixel level for each year.

Allocation of Forestation Area to Each Tree Species: unlike forest fire, after allocating forest area to each pixel according to different forest types, we further apportioned the forestation area within each pixel based on the proportion of tree species. The forestation area for each tree species in each pixel was proportionally distributed based on the total forestation area of each forest type (Fig. 2b). The area proportions for each tree species within each forest type were determined by the tree species distribution at the provincial level, which was sourced from the literature (see the Excel file named 'Proportion of tree species.xlsx' in supplementary materials (https://data.mendeley.com/datasets/5kp76xww4r/3) for details). This method ensured that the forestation area was allocated to each tree species according to the provincial species composition and forest type distribution.

(c) Forest harvest

Determining the Distribution of Two Forest Harvest Types Annually: Since Harvest for Reforestation (HFRFT) is essentially the same as reforestation after harvest (RAH), its spatial distribution was identical to that of RAH. The distribution of harvest for other land use (HFOLU) was derived through land cover change analysis conducted over two-year intervals. After allocating the two forest harvest types spatially, each harvest pixel was categorized into one of the five forest types based on the land use/land cover dataset. This process ensured that each harvest area was correctly classified according to its forest type and land use characteristics.

Allocation of Wood Harvest Statistical Volume to Each Harvest Pixel Annually: The total harvested wood volume was allocated to the two harvest types based on their respective proportions (Fig. 2b). The proportion of each harvest type was calculated by dividing its pixel count by the total number of harvest pixels. Once the proportions were determined, the actual harvest volume for each pixel was allocated by evenly distributing the total volume of its respective harvest type across its corresponding pixel count. This ensured that the harvested wood

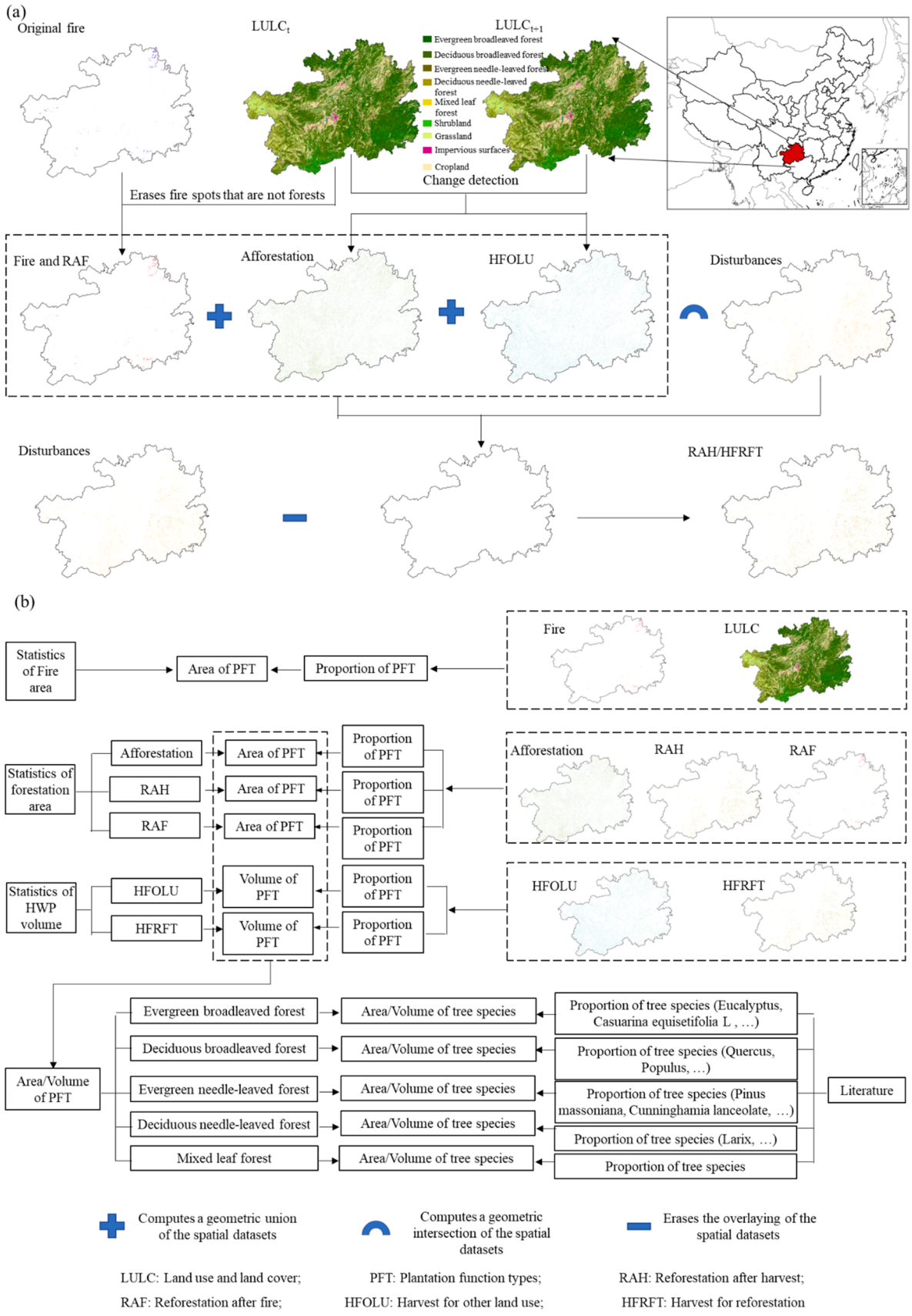

Fig. 2. Spatial distribution of FAFD (a), area allocation to PFT and tree species (b) (Note: Take Guizhou Province, China, as an example).

volume was accurately distributed across the spatially allocated harvest areas.

Allocation of Wood Harvest Statistical Volume to Each Tree Species: Consistent with the forestation process, once the volume from forest harvest was assigned to each pixel by forest type, we subsequently distributed the harvested volume per pixel among the corresponding tree species in proportion. The area proportions for each tree species within each forest type were determined by the species distribution at the provincial level, which was sourced from the literature (see the Excel file named 'Proportion of tree species.xlsx' for details). This method ensured that the wood harvest volume was distributed to each tree species according to its proportion within the respective forest type and province.

2.2.3. Localized Bookkeeping models and descriptions

The Bookkeeping model developed by Houghton et al. (1983) estimates changes in carbon storage by analyzing land cover change rates and the associated alterations in carbon accumulation per hectare in vegetation and soil. A key feature of the model is its ability to track carbon fluxes resulting from both human activities and natural disturbances. This is achieved by defining response curves that represent carbon changes in live vegetation biomass, dead vegetation biomass, harvested wood products, and soil (Houghton and Nassikas, 2017).

In this study, vegetation carbon pools were divided into four main categories: (1) live vegetation carbon pool, which includes afforestation, RAH and RAF; (2) dead vegetation carbon pool, representing on-site dead biomass due to harvest or fire; (3) harvested wood product (HWP) carbon pool; and (4) combustion carbon pool, namely the directly released carbon by fire (Fig. 1). Due to significant uncertainties in soil carbon, this study focused solely on carbon sequestration and emissions related to forest vegetation.

The annual change in the forest vegetation carbon pool was expressed as:

$$\Delta VC_t = \sum_{t=1}^{Min(T,N)} (\Delta LVC_t + \Delta WPC_t + \Delta DVC_t + \Delta BVC_t) \quad (1)$$

where ΔVC_t is the annual change of forest vegetation carbon pool for FAFD, ΔLVC_t is the change of living vegetation carbon pool, ΔWPC_t is the change of HWP carbon pool, ΔDVC_t is the change of dead vegetation carbon pool, and ΔBVC_t is the change of vegetation combustion carbon pool. T represents the maturity period of the vegetation, and N is the study period.

(1) Forestation: Six growth models (Piecewise linear, Logistics, Hossfeld, Korf, and two Richards curves) were used to simulate tree growth across provinces (Fig. 3a). Parameters *a, b*, and *c* (Table 2) for six S-shaped growth curves were derived from previous studies, which fitted these curves based on forest resource inventory data across regions (Li, 2011; Lu et al., 2019; Xu et al., 2010). Protection plantations were assumed to stop sequestering carbon after reaching maturity, while other plantations were harvested at rotation age. Final results were averaged across the six models to reduce error and produced the corresponding standard deviation. The carbon budget for forestation only considered ΔLVC_t, with ΔWPC_t and ΔDVC_t setting as zero as it was already calculated in forestation harvest section. The ΔLVC_t for forestation was calculated as:

$$\Delta LVC_t = A_t \times \Delta VD_t \quad (2)$$

$$\Delta VD_t = (VD_{t1} - VD_{t2})/(t1 - t2) \quad (3)$$

Where A_t is the forestation area, and ΔVD_t is the change in vegetation carbon density between two consecutive age stages with VD_{t1} and VD_{t2}

Table 2
Description of different growth curves.

Model	Formula	source	Note
Richard	$VD = a\times(1\text{-}\exp(\text{-}b\times T))\hat{}c$	Pienaar (1973)	*VD* is the vegetation carbon density (t/ha), and T is the forest age (years). a, b, and c are growth curve parameters. a1, b1, and a2, b2, and a3, b3, and a4, b4 indicate parameters of young forest, middle forest, near-mature forest and mature forest, respectively.
Logistics	$VD = a/(1+b\times\exp(\text{-}c\times T))$	Von Gadow (1998)	
Hossfeld	$VD = a/(1+b/T\hat{}c)$	Zeide (1993)	
Korf	$VD = a\times\exp(\text{-}b/T\hat{}c)$	Zeide (1989)	
Piecewise linear	$VD = \begin{cases} a1\times T+b1 \\ a2\times T+b2 \\ a3\times T+b3 \\ a4\times T+b4 \end{cases}$	Chen et al. (2016)	

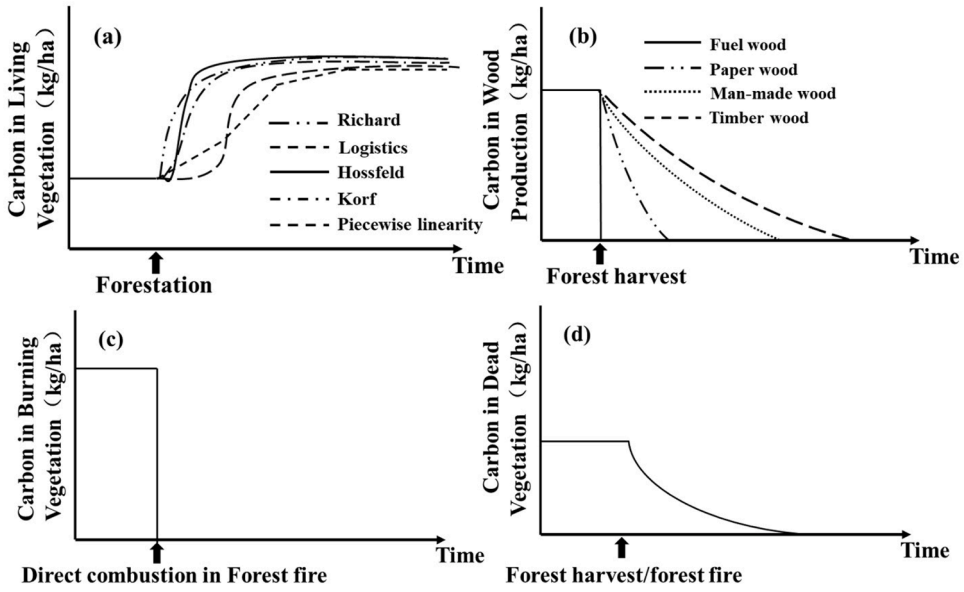

Fig. 3. Vegetation carbon response curves of FAFD: changes in vegetation carbon storage of forestation, reforestation after harvest and fire (a); changes in carbon stocks of forest harvested wood products (b); changes in carbon stocks of forest after direct combustion (c); changes in carbon stocks of dead vegetation from harvest and forest fire (d). (Modified from Chen et al. (2016)).

representing carbon densities at years *t1* and *t2*.

(2) Forest harvest: the carbon budget for forest harvest included ΔWPC_t and ΔDVC_t, excluding ΔLVC_t as regrowth was considered under forestation section. HWPs were divided into man-made wood, timber wood, paper wood, and fuelwood, with the first three decaying exponentially (Wang et al., 2024). Fuelwood emissions were completed within one year (Fig. 3b).ΔWPC_t was calculated by:

$$\Delta WPC_t = C_{(t)} + \mathrm{Inflow(t)} - C_{(t+1)} \quad (4)$$

$$C_{(t+1)} = \mathrm{e}^{-k} \times C_{(t)} + \left(1 - \mathrm{e}^{-k}\right)/k \times \mathrm{Inflow(t)} \quad (5)$$

$$\mathrm{Inflow(t)} = H_t \times D \times CF \quad (6)$$

Where $C_{(t)}$ and $C_{(t+1)}$ are the HWP carbon stocks in year t and t+1, respectively; k is the decay constant, calculated as k=$ln2/t_{HL}$, where t_{HL} is the half-life span of wood product; and Inflow(t) is the newly added HWP carbon stock in year t, H_t represents the HWP volume in year t, D is the basic wood density, and CF is the carbon fraction.

This study assumed that dead vegetation left on site after harvest released carbon ($\Delta DVC_{,t}$) into the atmosphere exponentially over time (Chen et al., 2016) (Fig. 3d):

$$\Delta DVC = H_t \times D \times CF \times \ (1/HE - 1) \ \times \ \left(1 - e^{-k'T'}\right) \quad (7)$$

where T', k' are the decomposition time and constant, respectively. And HE is the harvest efficiency. It is worth noting that the parameters of the above formula were divided into three types: maximum, medium and minimum, so final results were the average of the three types parameters with the corresponding standard deviation.

(3) Forest fire: Forest fire carbon budgets included ΔBVC_t and ΔDVC_t, with ΔLVC_t setting as zero as it was already included in the forestation section. Fire released carbon directly, and the remaining dead vegetation decomposed exponentially (Fig. 3d). The equations were:

$$\Delta BVC_t = A_t \times VD \times CE \times F_{above} \quad (8)$$

$$\Delta DVC_t = A_t \times VD_t \times F_{above} \times \ (1 - CE) \ \times \left(1 - e^{-k'T'}\right) \quad (9)$$

where A_t is burned area, VD is the vegetation carbon density during the fire, CE is the combustion efficiency, F_{above} is the proportion of aboveground biomass to the total vegetation, and $F_{above} = 1/(1+R)$ (R is the ratio of root to stem). The release time T' is assumed same as that for dead vegetation after harvest. Forest fire carbon budget results were also averaged across the results of three type of parameterizations to reduce error and produce the corresponding standard deviation.

2.2.4. Spatially modelling

This study modeled the carbon budget of each forest activity and fire disturbance type at the pixel level. The generated pixel data of forestation area for the three forestation types, wood product volume and forest fire area as described in Section 2.2.2 was implemented in the pixel-based modelling with corresponding localized parameters as described in Section 2.2.3.

3. Result

3.1. Total carbon budget from forest activities and fire disturbance

The total carbon budget of FAFD from 1986 to 2020 indicated a net carbon sequestration of approximately 710.64 ± 136.4 Tg C (Table 3) (the SD indicated cumulative estimates calculated by summarizing the average value of different methods). Significant differences were noted among different FAFD (Fig. 4a, b). Forestation was the major contributor to carbon sequestration, with an estimated 1529.36 ± 202.59 Tg C (Table 3). On the other hand, forest fire and harvest were the primary sources of carbon emissions, contributing 30% (233.34 ± 36.28 Tg C) and 70% (585.38 ± 29.91 Tg C) of emissions, respectively. Most regions showed net carbon sequestration, except the East region, which had net emissions of 33.85 ± 27.87 Tg C (Table 3). The Southwest region led in the highest carbon sequestration (290.04 ± 69.63 Tg C), followed by the Northwest region with carbon sequestration at 230.13 ± 51.99 Tg C. Spatially, the national average carbon sequestration density from FAFD was 172.95 Mg C km^{-2} (Fig. 4e), with notable regional differences. Sequestrations were concentrated in southwestern, northern, and northwestern China, while emissions were concentrated in eastern, southern China, the Greater Khingan Range, and Tibet.

Provincial results revealed that Chongqing had the highest carbon sequestration from forestation (88.16 Tg C), while Tianjin had the lowest (2.07 Tg C). Jiangsu showed the highest emissions (43.09 Tg C), and Beijing the lowest (1.43 Tg C) (Fig. 4f). Jiangxi and Hunan had strong carbon sequestration (500 to 2000 Mg C km^{-2}), contrasting with the weak carbon emission (0 to 500 Mg C km^{-2}) in Fujian, Guangdong, Guangxi, and Zhejiang. This difference was attributed to Jiangxi and Hunan's extensive forestation and lower harvest and fire impact, while the latter provinces had higher harvest and fire-affected areas (Fig S1a-c).

From 1986 to 1989, the national carbon budget indicated a net weak emission, transitioning to net sequestration from 1989 onwards, rising from 5.42 Tg C to 35.32 Tg C (Fig. 4g). This trend was supported by increased sequestration from forestation and reduced carbon emissions from harvested wood products. The Southwest and Northwest regions consistently showed increasing net sequestration, driven by large forestation areas (Table S1). The North region experienced emissions

Table 3
Total carbon budget from FAFD in China from 1986 to 2020 (unit: Tg C).

	North	Northeast	East	Southcentral	Southwest	Northwest	China
Forest fire							
BVC	24.86±3.03	22.97±0.11	9.97±3.79	6.94±2.56	9.45±2.14	0.88±0.06	75.07±11.68
DVC	52.39±6.43	48.7±0.22	21.15±8.04	14.66±5.41	19.59±4.4	1.79±0.12	158.28±24.61
VC	77.25±9.46	71.68±0.32	31.12±11.83	21.61±7.97	29.04±6.54	2.66±0.18	233.34±36.28
Forest harvest							
WPC	26.81±2.15	29.33±2.77	106.33±8.16	70.85±5.28	23.49±1.73	2.88±0.21	259.68±20.3
DVC	49.28±2.14	30.92±1.06	137.04±4.56	86.15±0.8	19.89±0.98	2.44±0.12	325.7±9.61
VC	76.08±4.28	60.24±3.83	243.37±12.72	157±6.08	43.38±2.71	5.31±0.32	585.38±29.91
Forestation							
LVC/VC	-301.76±101.64	-151.71±29.69	-240.64±52.42	-234.7±60.52	-362.46±78.88	-238.1±52.49	-1529.36±202.59
Total FAFD	-148.43±87.9	-19.79±25.54	33.85±27.87	-56.09±46.47	-290.04±69.63	-230.13±51.99	-710.64±136.4

Note: ΔLVC_t is the change of living vegetation carbon pool, ΔWPC_t is the change of HWP carbon pool, ΔDVC_t is the change of dead vegetation carbon pool, and ΔBVC_t is the change of vegetation combustion carbon pool. Forestation SD: reflecting the variation across six growth-curve models, Harvest/Fire SD: reflecting the variation across parameter sets (min/medium/max) for emission factors

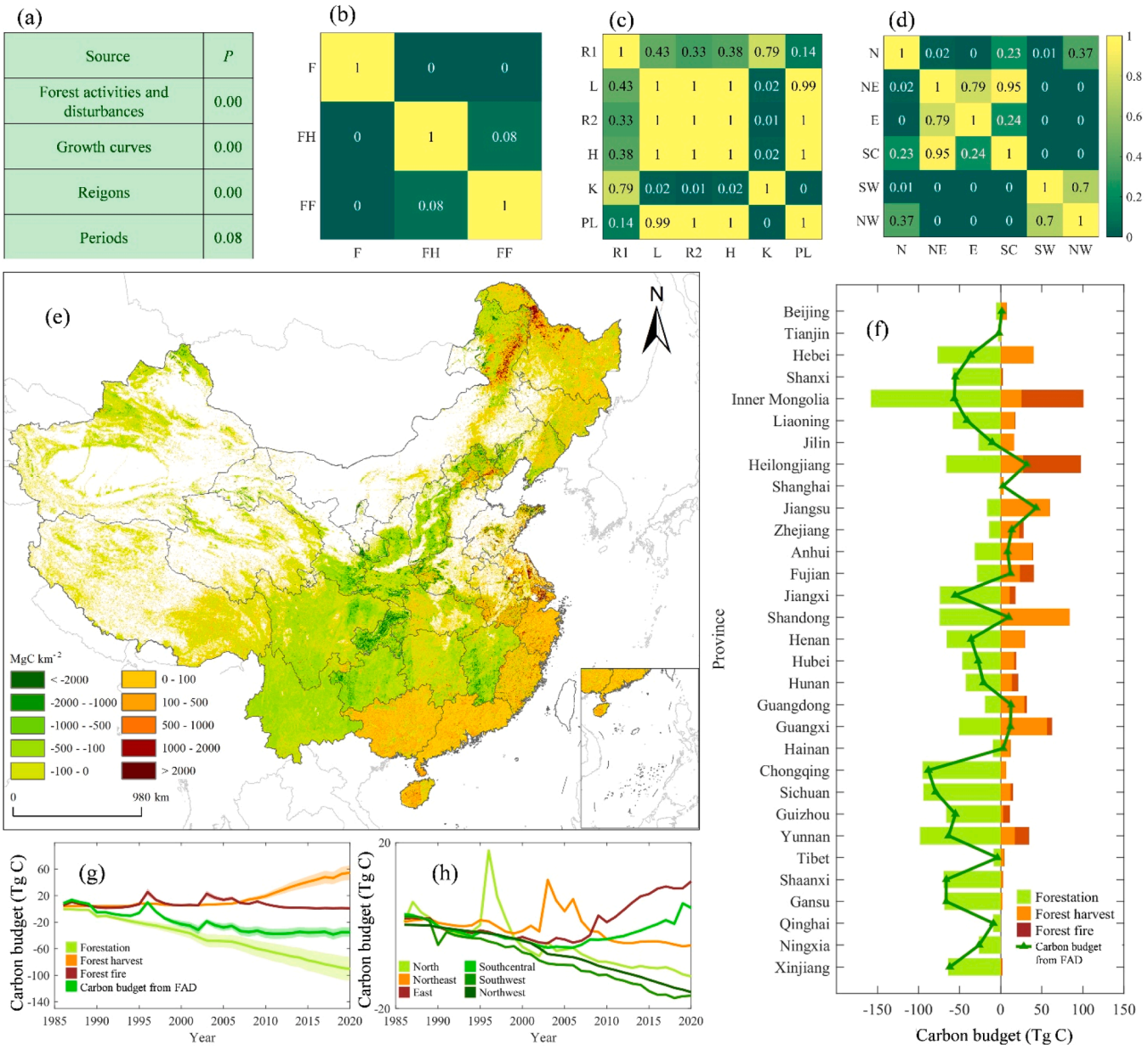

Fig. 4. Carbon budget from FAFD at a national scale (a-d. Multiple comparisons and ex-post comparisons of carbon budget from different FAFD types, growth curves, regions, and periods; e. spatial distribution of carbon budget; f. Provincial carbon budget; g-h. Annual carbon budget. Negative values indicate carbon sequestration, positive values represent emissions. Nodata for Taiwan Province, Hongkong and Macao. Abbreviations: F (Forestation), FH (Forest Harvest), FF (Forest Fire); R1 (Richar1), L (Logistic), R2 (Richar2), H (Hossfeld), K (Korf), PL (Piecewise Linear); N (North), NE (Northeast), E (East), SC (Southcentral), SW (Southwest), NW (Northwest). Map lines delineate study areas and do not necessarily depict accepted national boundaries.).

from 1986 to 2000, peaking in 1996 at 18.03 Tg C due to the major fire (1.04×10^6 ha, contributing 9.27% to total fire emission and offsetting 1.41% to the total carbon sequestration from forestation (Table 6)) in Inner Mongolia Province, followed by stable sequestration growth. Similarly, spikes in Northeast China (orange line, 2003 and 2006) were driven by large fires in Heilongjiang Province (burned areas: 2.87 × 105 ha and 3.26 × 105 ha, respectively), accounting for 6.52% and 4.5% of total fire carbon emission, respectively (Table 6). The Southcentral and East regions showed sequestration trends before 2010, shifting to emissions after (Fig. 4h), likely due to an emission rise from harvested wood product (Fig. S1f).

3.2. Carbon sequestration from forestation

During the period 1986-2020, forestation contributed to total carbon sequestration of 1529.36±202.59 Tg C, averaging 43.7±25.79 Tg C yr^{-1} (Table 4) (the SD indicated cumulative estimates calculated by summarizing the average value of six growth-curve models). Among the three forestation types, afforestation was the dominant contributor, accounting for 82.41% of the total sequestration, while RAF and RAH contributed 12.15% and 5.44%, respectively. Notably, carbon sequestration from RAF was approximately double that from RAH. The sequestration from afforestation showed a gradual increase with an annual growth rate of 36.01 ± 4.53 Tg C, attributed to the expansion of afforestation areas supported by ecological conservation projects. In contrast, RAF and RAH showed a decline in carbon sequestration trends post-2000, likely due to reduced reforestation areas (Fig. 5a).

Regionally, the Southwest region accounted for the highest proportion of carbon sequestration at 23.7%, followed by the Southcentral region at 15.35%. The Northeast region had the lowest contribution

Table 4
Total carbon sequestrations from forestation in China from 1986 to 2020 (unit: Tg C; SD: variation across six growth-curve models).

	North	Northeast	East	Southcentral	Southwest	Northwest	China
Types of forests based on use							
Protection plantation	-207.44±81.15	-66.82±17.2	-60.87±14.38	-69.47±15.63	-169.24±40.04	-142.01±29.76	-715.85±114.06
Timber plantation	-53.15±15.49	-64.74±9.82	-120.64±33.84	-101.82±23.38	-106.59±21.15	-30.98±6.94	-477.91±67.04
Economic plantation	-38.8±9.32	-16.69±4.7	-49.76±12.34	-61.28±13.46	-82.29±17.79	-56.83±15.6	-305.64±38.85
Fuel plantation	-2.37±1.11	-3.46±1.56	-3.44±0.58	-8.07±1.86	-4.35±1.12	-8.27±2.04	-29.97±4.07
Forestation methods							
Afforestation	-242.03±70.4	-116.08±24.42	-184.93±39.55	-194.35±50.31	-292.57±58.47	-230.4±51.52	-1260.37±158.56
Reforestation after Harvest	-8.36±2.56	-9.37±2.37	-24.57±6.05	-15.54±3.78	-20.32±5.33	-4.95±1.06	-83.13±12.2
Reforestation after fire	-51.36±30.73	-26.26±4.42	-31.15±7.53	-24.8±6.96	-49.56±16.6	-2.74±0.6	-185.87±42.22
Total forestation	-301.76±101.64	-151.71±29.69	-240.64±52.42	-234.7±60.52	-362.46±78.88	-238.1±52.49	-1529.36±202.59

(9.92%) due to its smaller forestation area of 133.73 × 10^4 ha (Table S1). Temporally, all regions exhibited a consistent increase in carbon sequestration (Fig. 5b).

Among forest use types, protection plantations led with 715.85 Tg C, representing over 40% of total forestation carbon sequestration. Timber plantations and economic plantations followed, contributing 31.25% and 19.98%, respectively, while fuel plantations had the least contribution at 1.96%. The carbon sequestration of protection, timber, and economic plantations showed rapid growth, whereas fuel plantations grew slowly throughout the period (Fig. 5c).

Spatial results showed that the average carbon sequestration density from forestation was -238.45 Mg C km^{-2}. This density was higher in central and western China (500 to -3000 Mg C km^{-2}) and lower in eastern and northwestern China (0 to 500 Mg C km^{-2}) (Fig. 5d). This spatial distribution was primarily driven by afforestation, which had an average density of 208.18 Mg C km^{-2} (Fig. 5e). RAH had a higher carbon sequestration density in southeastern China, due to significant timber plantation areas planted between 1986 and 2020 (Fig. 5f). The southwestern, northeastern, and southeastern China showed strong carbon sequestration densities from RAF (50 to -1000 Mg C km^{-2}), corresponding to substantial RAF areas (Fig. 5g).

3.3. Carbon emission from forest harvest

Carbon emission from forest harvest was 585.38±29.91 Tg C, with an emission rate of 16.73±0.85 Tg C yr^{-1} (Table 5) (the SD indicated cumulative estimates calculated by summarizing the average value of different parameter sets). Of these emissions, 44.29% came from HWP, while 55.71% originated from decomposing dead vegetation left on-site. Emissions from forest harvest largely stemmed from harvested forest and other land use (HFOLU), which contributed 92.06% (538.90 Tg C) of the emissions, in contrast to harvested forest after reforestation and afforestation (HFRAH), which contributed 7.94% (46.47 Tg C). This discrepancy was primarily due to the significantly larger volume of HWP under HFOLU, nearly ten times that of HFRAH (Fig. S2b). Over time, emissions from forest harvest exhibited an exponential increase, mainly driven by HFOLU (Fig. 6a).

HWP-specific carbon emissions totaled 259.68 ± 20.3 Tg C, with an emission rate of 7.42 ± 0.58 Tg C yr^{-1} (Table 5). The East and Southcentral regions accounted for nearly 70% (177.18 Tg C) of these emissions due to higher HWP production. Among HWP types, man-made wood contributed the most, around 50% (131.64 Tg C) of total HWP emissions. Despite the volume of timber wood products were much higher than that of fuel wood, their emissions were similar due to timber wood's slower decomposition rate. Paper wood had the smallest contribution (3%) due to its lower stock. The emissions from all HWP types showed an accelerating trend (Fig. 6c). Notably, the carbon emissions from decomposing dead vegetation exceeded those from HWP, reaching 325.7 Tg C, with an emission rate of 5.95 Tg C yr^{-1} (Table 5). This was due to the quicker carbon release rate from decomposing vegetation compared to the slower release from HWP. Additionally, durable wood products like furniture (lifespan over 50 years) helped sequester carbon and contributed minimally to emissions during this period.

Spatially, forest harvest produced an average carbon emission density of 92.04 Mg C km^{-2} (Fig. 6d). HFOLU emissions were most significant in eastern and southern China (50–1500 Mg C km^{-2}) and lowest in western China (0–50 Mg C km^{-2}), aligning with lower land conversion rates and smaller HWP volumes in the west. The spatial pattern of HFOLU emissions mirrored the total forest harvest emissions, averaging 89.69 Mg C km^{-2} and forming the main contribution to overall emission density (Fig. 6e). HFRFT emission density showed a similar but smaller pattern, averaging 14.57 Mg C km^{-2} (Fig. 6f). Provinces such as Guangdong, Fujian, Zhejiang, Guangxi, and Anhui, where extensive plantations of species like *eucalyptus* and *Cunninghamia lanceolata* exist, had the highest emission densities, contributing over 50% of total emissions (Fig. 4f). The Northwest region, home to significant reforestation efforts under the Three-North Shelter Forest Project (272.17 × 10^4 ha, 16% of total forestation), showed minimal carbon emissions (0–50 Mg C km^{-2}).

3.4. Carbon emission from forest fire

The total carbon emissions from forest fire ranged from 189.06 to 233.34±36.28 Tg C, with approximately 30% released through direct combustion and about 70% from the decomposition of dead vegetation left on the site (Table 3) (the SD indicated cumulative estimates calculated by summarizing the average value of different parameter sets). The carbon emission from forest fire exhibited significant interannual variability, generally showing a decreasing trend. Notable peaks in emissions were recorded in 1987, 1996, 2003, 2006 and 2009, together comprising roughly 39.37% of total emissions over the study period (Fig. 7b). The year of 1996 represented the most significant impact, contributing 10.85% of emissions and offsetting 1.65% of forestation carbon sequestration, primarily due to large-scale forest fires in Inner Mongolia that alone accounted for 9.27% of emissions and 1.41% of sequestration offset (Table 6). The year of 2003 followed closely, responsible for 9.74% of emissions and 1.48% of forestation carbon sequestration offset, driven by major fire events in Heilongjiang Province (6.52% emissions, 0.99% offset) and Inner Mongolia (1.90% emissions, 0.29% offset) (Table 6). This decline in emissions suggested that government fire prevention and control strategies were effective. The North and Northeast regions were the highest contributors, with emissions of 77.25 Tg C and 71.68 Tg C respectively, each representing about 30% of the total emissions (Table 3). The Southwest and East regions had similar contributions at around 13% each (29.04 Tg C and 31.12 Tg C), while the Northwest region had the lowest emissions (2.66 Tg C), reflecting its smaller burned area (Table 3). Carbon emissions from vegetation combustion specifically totaled 75.07 Tg C, with a rate of 2.14 Tg C yr^{-1}, while emissions from decomposing dead vegetation reached 158.28 Tg C (Table 3).

Spatially, the forest fire resulted in an average carbon emission

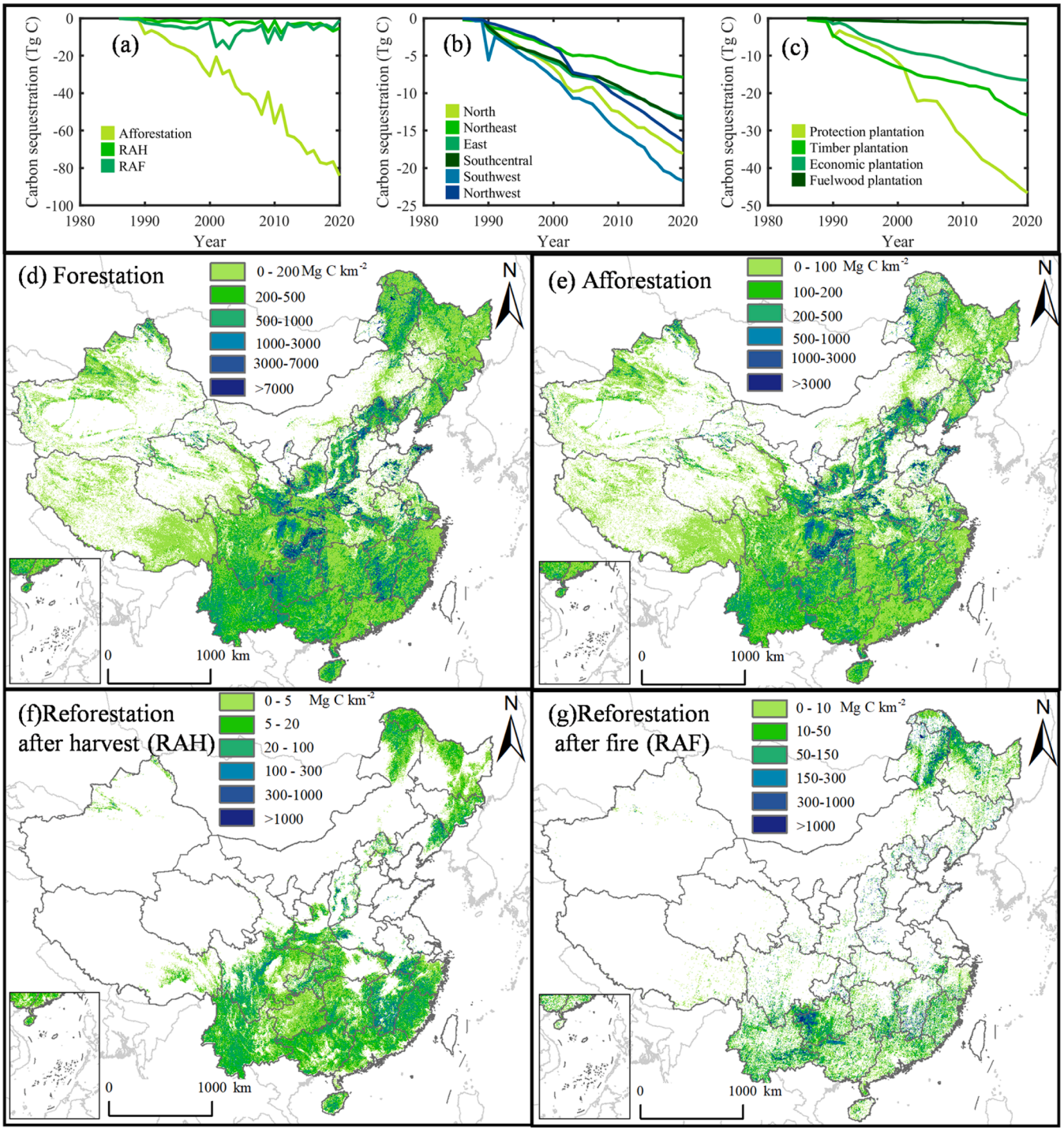

Fig. 5. Carbon sequestration from forestation (a-c: annual carbon sequestration of different forestation types, regions and plantation types; d-g: spatial distribution of carbon sequestration density from forestation, afforestation, RAH and RAF, respectively. Note: map lines delineate study areas and do not necessarily depict accepted national boundaries).

density of 142.42 Mg C km^{-2} (Fig. 7a). The carbon emission density was higher in the northeast and southeast of China (50-1500 Mg C km^{-2}), while lower in the other regions (0-50 Mg C km^{-2}) (Fig. 7a). Provincially, Heilongjiang and Inner Mongolia collectively contributed approximately 60% (146.22 Tg C) of the total carbon emissions.

3.5. Carbon budget of major tree species in forestation and forest harvest

At the national scale, *Populus*, *Cunninghamia lanceolata*, *Pinus massoniana*, and *Quercus* species were the primary carbon-sequestering trees, accounting for 25.13% (313.79 Tg C), 19.39% (204.62 Tg C), 17.45% (217.92 Tg C), and 11.09% (138.46 Tg C) of the total carbon sequestration, respectively (Fig. 8d and e). *Populus* had the highest impact, particularly in the East and Northwest, sequestering 96.77 Tg C and 87.60 Tg C, respectively. *Cunninghamia lanceolata* and *Pinus massoniana* were notable in the Southcentral, East, and Southwest regions. *Eucalyptus*, known for its fast growth and high yield, contributed 30.13 Tg C, mainly in the East and Southcentral, with Guangxi Province alone

Table 5
Total carbon emission from forest harvest in China (unit: Tg C; SD: variation across parameter sets (min/medium/max) for emission factors).

Region	Carbon stock types	Man-made wood	Paper wood	Fuel wood	Timber wood	Total wood
North	WPC	14.23 ±1.19	0.22 ±0.02	3.26 ±0.26	9.09 ±0.68	26.81 ±2.15
	DVC	24.63 ±1.09	0.73 ±0.02	1.45 ±0.11	22.47 ±0.91	49.28 ±2.14
	Total	38.86 ±2.28	0.95 ±0.04	4.71 ±0.37	31.56 ±1.59	76.09 ±4.29
Northeast	WPC	7.3 ±0.74	0.51 ±0.06	9.28 ±0.7	12.24 ±1.28	29.33 ±2.77
	DVC	10.84 ±0.34	0.83 ±0.01	4.57 ±0.33	14.68 ±0.38	30.92 ±1.06
	Total	18.14 ±1.08	1.34 ±0.07	13.85 ±1.03	26.92 ±1.66	60.25 ±3.83
East	WPC	66.42 ±4.5	1 ±0.09	25.71 ±2.58	13.2±1	106.33 ±8.16
	DVC	106.9 ±3.96	1.73 ±0.02	8.33 ±0.11	20.09 ±0.46	137.04 ±4.56
	Total	173.32 ±8.46	2.73 ±0.11	34.04 ±2.69	33.29 ±1.46	243.37 ±12.72
Southcentral	WPC	36.6 ±2.59	5.04 ±0.33	17.79 ±1.55	11.42 ±0.81	70.85 ±5.28
	DVC	56.84 ±0.74	7.71 ±0.07	5.32 ±0.05	16.28 ±0.08	86.15 ±0.8
	Total	93.44 ±3.33	12.75 ±0.4	23.11 ±1.6	27.7 ±0.89	157 ±6.08
Southwest	WPC	6.34 ±0.49	0.77 ±0.05	11.54 ±0.84	4.84 ±0.35	23.49 ±1.73
	DVC	8.26 ±0.4	1.24 ±0.08	3.31 ±0.17	7.07 ±0.33	19.89 ±0.98
	Total	14.6 ±0.89	2.01 ±0.13	14.85 ±1.01	11.91 ±0.68	43.38 ±2.71
Northwest	WPC	0.75 ±0.06	0.03 ±0.00	1.11 ±0.07	0.98 ±0.07	2.88 ±0.2
	DVC	0.84 ±0.05	0.05 ±0.00	0.49 ±0.02	1.05 ±0.05	2.44 ±0.12
	Total	1.59 ±0.11	0.08 ±0.00	1.6 ±0.09	2.03 ±0.12	5.32 ±0.32
China	WPC	131.64 ±9.57	7.58 ±0.54	68.69 ±6	51.76 ±4.19	259.68 ±20.3
	DVC	208.31 ±6.57	12.29 ±0.06	23.47 ±0.8	81.64 ±2.18	325.7 ±9.61
	Total	339.95 ±16.14	19.87 ±0.6	92.16 ±6.8	133.4 ±6.37	585.38 ±29.91

accounting for 16.19 Tg C (53.74% of the total for eucalyptus). *Quercus* and *Larix* played significant roles in the North and Northeast, contributing 11.08% (67.09 Tg C) and 14.97% (112.73 Tg C) of the total sequestration, respectively.

In terms of carbon emissions from forest harvest, *Pinus massoniana, Populus*, and *Quercus* were the main contributors, making up 17.56% (102.49 Tg C), 16.89% (98.54 Tg C), and 24.02% (140.21 Tg C) of total emissions, respectively. Emissions from *Pinus tabuliformis* and *Cupressus* were relatively small, at 0.56% and 3.00%. Regional differences were notable, with lower emissions from *Pinus massoniana* in the Southwest and from *Populus* and *Quercus* in the Northwest due to smaller harvest volumes. Eucalyptus emissions were significant in the Southcentral region (5% of total emissions) due to extensive planting. *Larix* contributed 3.28% (19.12 Tg C) of total emissions, with more than 80% occurring in the Northeast.

3.6. Carbon offset of forest harvest and fire

More than half (53.53%) of the carbon sequestered from forestation was offset by emissions from forest harvest and fire during 1986–2020. The impact of forest fire on carbon sequestration was generally small (under 20% in most regions), while forest harvest had a significant offset effect (over 30% in most regions). Nationally, forest harvest accounted for 38.28% of the offset, more than double that of forest fire (15.26%). The East region showed the highest offset disparity, while the Northwest had the smallest (Fig. 9c). Spatial variability in these offset effects was evident, with most areas showing less than 50% offset (Fig. 9a and b). However, in eastern, southern, and southeastern China, forest harvest offset reached 50% to 500% (Fig. 9a), with some areas in Jiangsu, Zhejiang, Fujian, Guangdong, and Guangxi exceeding 200% due to high-yield plantations (Fig. 9d). High offset effects from fire were seen in regions like the Greater Khingan Mountains, driven by frequent fire and events like the 1987 fire, which emitted 0.025-0.050 Pg C (Houghton and Hackler, 2003).

The offset effect of forestation carbon sequestration by carbon emissions from forest harvest varied across tree species, with an average offset effect of 42.52%. Notably, *Quercus* and *Eucalyptus* showed higher offset effects of 101.27% and 97.64%, respectively (Fig. 9d), largely due to their higher carbon emission from forest harvest (Fig. 9e). In contrast, *Pinus tabulaeformis* and *Larix* demonstrated minimal offset effects of only 3.51% and 10.23% (Fig. 9d), associated with lower harvest emission and higher carbon sequestration through forestation (Fig. 9e). Regionally, the offset effect of *Pinus massoniana* in East and Southcentral regions was ten times higher than in the Southwest region (Fig. 9g-i), reflecting the notably higher carbon sequestration rates from forestation in the latter region (Fig. 8f-h). *Larix* exhibited negligible offset effects in the North and Northwest regions, at 3.04% and 0.96%, respectively. In the Northeast, Southcentral, and East regions, *Quercus* demonstrated offset effects exceeding 100%, reaching 486.73% in the East, indicating a substantial offset impact. *Populus* exhibited relatively small offset effects of 1.13% to 21.34% across North, Northeast, Southcentral, and Northwest regions but a significantly higher effect in the East at 79.44% due to lower forestation sequestration. Principal timber species, *Cunninghamia lanceolata* and *Eucalyptus*, also varied regionally with the former having offset effects of 28.10% to 39.54% in East and Southcentral while the latter having offset effects ranging from 97.55% to 124.20% (Fig. 9g-h).

4. Discussion

4.1. Comparison with other estimates

Our estimated carbon sequestration from forestation ranges from 17.01 to 71.89 Tg C yr^{-1}, which is comparable to the range (20.50 to -53.25 Tg C yr^{-1}) from previous studies based on the inventory method (Fang et al., 2001; Guo et al., 2013; Xu et al., 2010; Yu et al., 2020) and empirical model method (Cheng et al., 2024) (Fig. 10a). Notably, our estimates during 1989-1998, 1989-2008, and 1989-2003 align closely with the findings from Fang et al. (2001), Guo et al. (2013), and Xu et al. (2010). Our result is around 20 Tg C yr^{-1} higher than Yu et al. (2020), which analyzed the carbon change based on 2748 planted forests sites at a nationwide field campaign between 2011 and 2015. This discrepancy arises primarily because Yu's study classifies subtropical plantations as coniferous forests (e.g., *Cunninghamia lanceolata* and *Pinus massoniana*). However, subtropical regions also contain extensive fast-growing broadleaf plantations, such as eucalyptus, which are not accounted for in this classification. Similarly, the result (50.83 Tg C yr^{-1}) exceeds that of Cheng et al. (2024) (40 Tg C yr^{-1}), which calculated the carbon storage using the age-carbon storage relation based on national forest inventory data, as it accounts for carbon sequestration from forests established before 1990.

Our estimated carbon emission from forest harvest during 1990-2004 is 0.75 Tg C yr^{-1}, which is much lower than the finding of Bai (2007) (14.77 Tg C yr^{-1}) using carbon stock-change approach, production approach and atmospheric-flow approach of estimating HWP carbon stock (Fig. 10b). This large discrepancy may be explained by the assumption difference in carbon emission of forest products. Bai (2007) assumes the carbon release of forest products is linear with its lifespan, causing large carbon emission in the earlier years. In contrast, this study assumes the carbon release increases with the age of use. Similarly, our

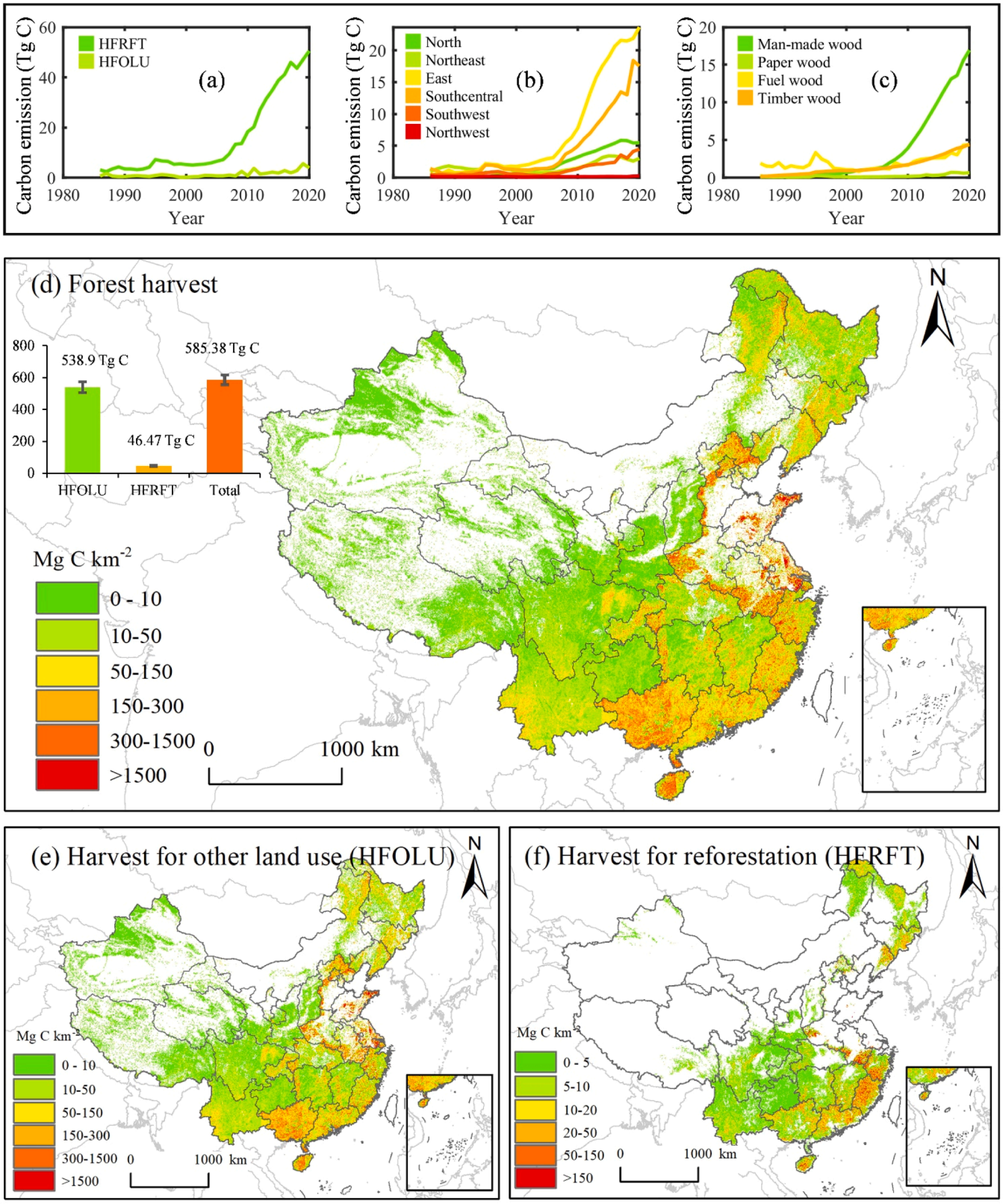

Fig. 6. Carbon emission from forest harvest (a-c: annual carbon emission in different harvest type, region and forest type, respectively; d-f: spatial distribution of carbon density from forest harvest, harvest for other land use and harvest for reforestation, respectively. Note: map lines delineate study areas and do not necessarily depict accepted national boundaries).

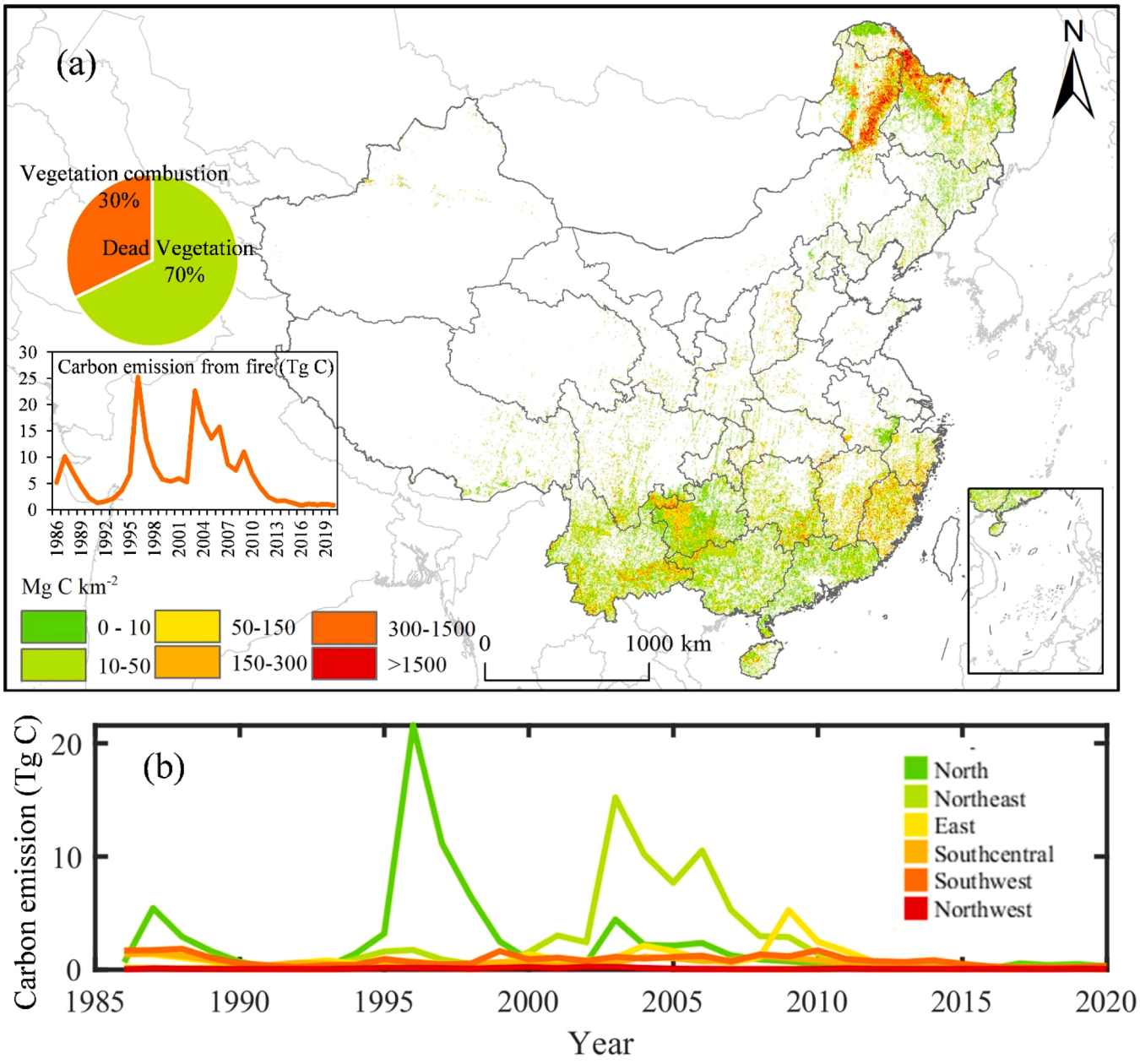

Fig. 7. Distribution of carbon emission from forest fire (a) and annual carbon emission from total forest fire process in six regions (b) (Note: map lines delineate study areas and do not necessarily depict accepted national boundaries).

forest harvest carbon emission during 2000-2020 (10.54 Tg C yr^{-1}) is also lower than that from Wang et al. (2024) (20.80 Tg C yr^{-1}) using a first-order decay method. This is mainly due to the differences in the assumed lifespan of product usage. It is also worth noting that our estimated emission rate during 1999-2008 (3.61 Tg C yr^{-1}) is around two times larger than the results reported by Lun et al. (2012) (1.98 Tg C yr^{-1}) using a carbon stock-change approach. The main reason is that Lun et al. (2012) assumes no carbon release during the usage of products. Our estimated emissions from forest fire (0.30-2.70 Tg C yr^{-1}) overall align well with previous studies which used emission factor method (China Academy of Science, 2023; Tian et al., 2003; Fan et al., 2024) or analyzed volumes of stem loss from forest fire (Zhang et al., 2016) (1.00-3.60 Tg C yr^{-1}) (Fig. 10c). The estimation is lower than that of Fan et al. (2024) mainly due to the different sources of vegetation carbon density. The used vegetation carbon density of Fan et al. (2024) is derived from remote sensing products of ESA, resulting in a significantly higher estimate (Fig. 10c).

4.2. Reliability of the estimated carbon budget using localized Bookkeeping model

It is worthy noted that the validation of carbon budget from three FAFD types is challenging due to the lack of corresponding long-term CO_2 monitoring data. For the part of carbon sequestration from forestation, one way to validate our results is to compare with existing results from previous studies which estimated carbon sequestration based on forest inventory data. Results show that our estimates of forestation carbon sequestration align closely with previous studies using plot-based inventory method at national scale (Fig. 10a) (Fang, et al., 2001; Xu et al., 2010; Guo et al., 2013; Cheng et al., 2024) and also provincial scale with a high validation accuracy (R^2 = 0.69) (Fig. 11) (Zhang, 2009; Guan et al., 2016; Han and Liang, 2015; Liu et al., 2017; Jiao and Hu, 2005; Jia, 2014; Li, 2015; Wu et al., 2019; Zhang et al., 2025; Ma, 2024; Liu, 2015; Zhang et al., 2018; Wang 2014; Li, 2012). Given that forest inventory is a well-established method for estimating

Table 6
The contribution from major fire on total carbon budget during 1986-2020.

Contribution of major fire at total fire carbon emission	1987	1995	1996	2003	2006	2009
China	4.36%	2.90%	10.85%	9.74%	6.77%	4.74%
The North region	2.33%	1.36%	9.28%	1.90%	1.01%	
The Northeast region		0.68%		6.53%	4.52%	
The East region						2.25%
Inner Mongolia Province	2.32%	1.34%	9.27%	1.90%	0.96%	
Heilongjiang Province				6.52%	4.50%	
Fujian Province						2.00%
Contribution of maior fire at total carbon budget	1987	1995	1996	2003	2006	2009
China	0.66%	0.44%	1.65%	1.48%	1.03%	0.72%
The North region	0.36%	0.21%	1.41%	0.29%	0.15%	
The Northeast region		0.10%		1.00%	0.69%	
The East region						0.72%
Inner Mongolia Province	0.35%	0.20%	1.41%	0.29%	0.15%	
Heilongjiang Province				0.99%	0.69%	
Fujian Province						0.30%

forest carbon stocks (Piao et al., 2022), this consistency supports the reliability of our results.

Validating carbon emissions from forest fires directly is extremely challenging, as pre- and post-fire biomass measurement requires unpredictable pre-fire surveys and is impractical beyond site scale. Similarly, validating emissions from post-harvest dead vegetation decomposition and harvested wood product (HWP) oxidation requires prohibitively complex controlled experiments. Consequently, (1) for fire emissions, we employed the widely accepted emission factor method (IPCC, 2006; van der Werf et al., 2010; Binte Shahid et al., 2024; Dobosz et al., 2025), which is recognized as a robust alternative with direct field measurement (Akagi et al., 2011; Bougma et al., 2023; Wang et al., 2022) and fire emission estimates are compared to existing regional studies (Fig. 10c); (2) For decomposition and HWP emissions, IPCC guidelines are followed with key refinements: exponential decay replaces linear assumptions for dead vegetation, and the first-order decay (FOD) method is used for HWPs (Harmon et al., 2020; IPCC, 2006; Spear and Hart, 2025; Wu et al., 2025; Zhou et al., 2023)). Utilizing these established, guideline-based methodologies represents a practical and accepted alternative in the absence of direct verification.

4.3. Uncertainty and future direction

To quantify the uncertainty of method for allocating area or volume (section 2.2.2), an experiment was further conducted by assuming the fire-affected area as the vegetation type with either the largest or smallest area proportion within each province. Similar experiments were also conducted for forestation area and harvest volume. The change ratio was then calculated, comparing with the normal scenario results. Results showed that the change ratio was relatively small, ranging from 5.43% to 7.11% for forestation, 1.26% to 2.51% for forest fire, and 0.07% to 10.21% for forest harvest (Table S2). Therefore, the uncertainty of area and volume allocation method used in this study is limited.

The main uncertainty in carbon sequestration estimation from forestation arises from parameter discrepancies among different growth curves. The carbon sequestration estimates vary significantly across the six curves (Fig. 3a; Fig. 12), with the highest estimate from the piecewise linear curve exceeding the lowest from the Korf curve by 564.58 Tg C between 1986 and 2020. This study averaged the carbon sequestration estimates from all six curves to minimize errors caused by parameter variability. Limited to the data availability, growth curve parameters were only distinguished between southern and northern China, lacking provincial-level refinement. This may lead to discrepancies in representing actual carbon density for specific tree species.

For forest harvest, the decay coefficient, which determines carbon release rates from forest products, is based on IPCC national-level data, but we minimized uncertainty by province- and species-specific wood density, carbon fractions, and harvest coefficients, with climate-zone decomposition rates. This could introduce regional and provincial biases in carbon release estimates. We have reduced the uncertainty of vegetation types by using provincial-level carbon densities for five functional vegetation types. However, in forest fire analysis, burning efficiency and decomposition coefficients, which vary by tree species, are generalized by plant function types as coniferous or broadleaf due to the poor data accessibility, potentially biasing the total carbon emission estimates.

Future parameterization efforts should focus on deepening the understanding of plant growth responses and carbon release processes. Incorporating longer, more consistent time series and higher-resolution spatial datasets is crucial to improve the accuracy of the simulated budget. The spatialized Bookkeeping model can integrate land cover, forest disturbance, and fire distribution data to map the spatial distribution of forest activities and track carbon stock changes.

The increase in forest carbon sequestration in China over the past decade has been mainly attributed to climate change, ecological restoration projects, and forest management (Fang et al., 2018). This study examines the impact of land management (such as forestation and forest harvest) and fire disturbance on forest carbon sequestration in China, but does not consider the effects of climate change and other anthropogenic management practices (such as agricultural management). Tang et al. (2018) found that warming can enhance the gross primary productivity (GPP) of China's forests, but this does not necessarily lead to an increase in carbon stocks. Under extreme climatic conditions (such as drought), tree mortality can result in a decline in forest productivity and carbon stocks (Anderegg et al., 2015; Peng et al., 2011; Vicente-Serrano et al., 2013; Allen et al., 2010). Long-term plot monitoring data from the Changbai Mountain aging forests over 30 years showed that climate warming has led to a reduction of 7.3 Mg C hm^{-2} in carbon sequestration in spruce and fir forests, and a reduction of 0.96 Mg C hm^{-2} in red pine-broadleaf mixed forests (Dai et al., 2013). Li et al. (2021) found that the subtropical forests in southern China were carbon sinks from 2003 to 2016, but became a strong carbon source during the drought years of 2011-2013. The other anthropogenic management practices (pest and disease control, understory vegetation management, intercropping, thinning, and fertilization) interventions significantly influence forest carbon stock dynamics (Yu et al., 2024; Fang et al., 2018; Pan et al., 2011). Recent studies demonstrate that moderate thinning (retaining 60-70% stand density) can substantially enhance the growth of dominant trees, increasing aboveground biomass carbon stocks by 19-28% (Yu et al., 2024). Conversely, the removal of understory ferns has been shown to reduce microbial carbon use efficiency and carbon accumulation, leading to an approximate 22% decline in carbon storage (Saponaro et al., 2025). Pest and disease outbreaks offset 3.1% of China's forest biomass carbon sequestration (Liu et al., 2020), while fertilization combined with dry-season irrigation can boost carbon storage in eucalyptus plantations by 37.4% (Yang et al., 2023). Additionally, understory vegetation conversion in Chinese hickory plantations increased soil carbon stocks by approximately 15% (Deng et al., 2023). Therefore, future efforts should be towards to integrating the comprehensive effects from climate change and other anthropogenic management factors.

4.4. Implications and future strategies

Our estimates indicate stronger carbon sequestration from forest

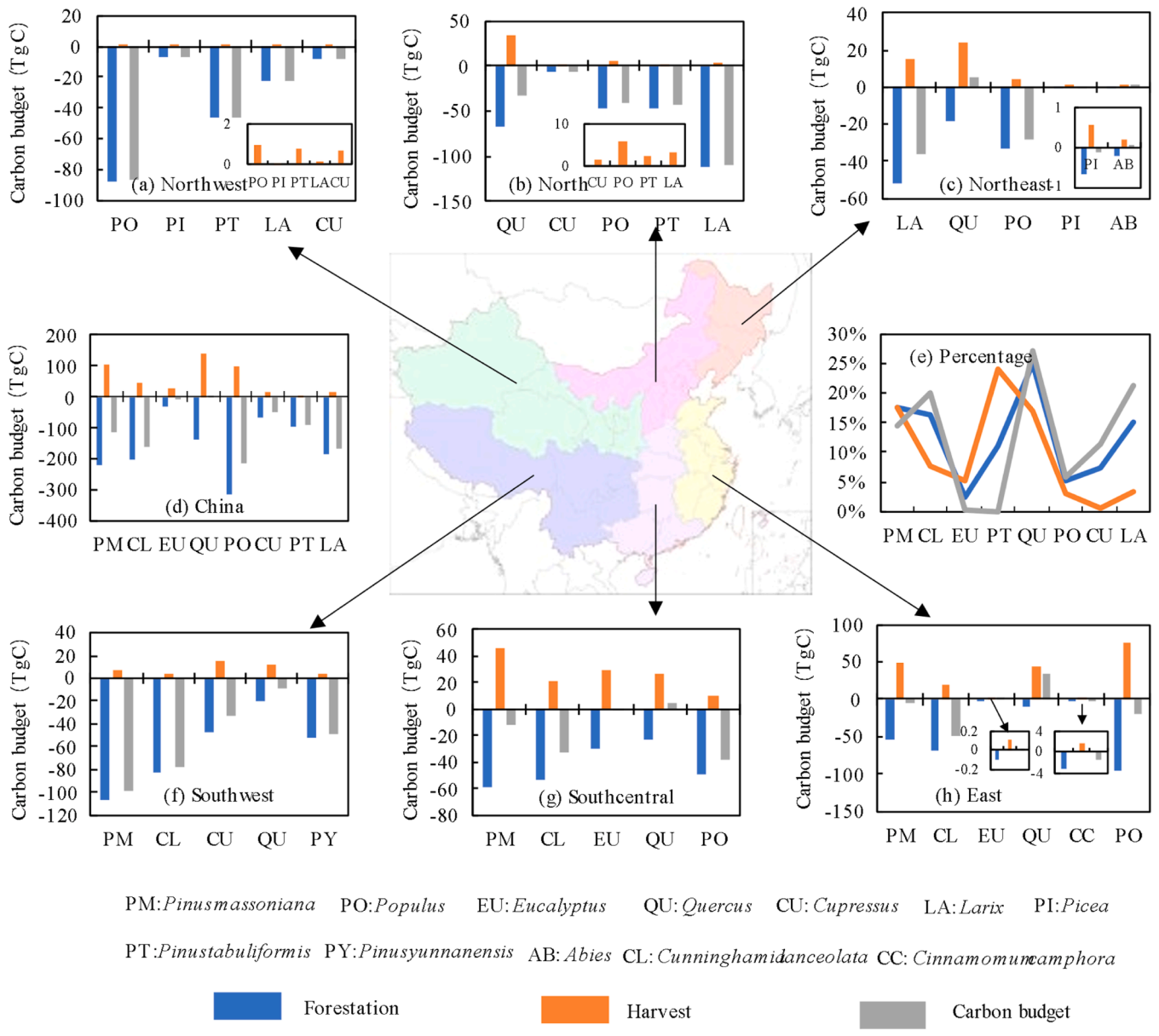

Fig. 8. Carbon budget from forestation and forest harvest in different tree species in China from 1986-2020 (Note: map lines delineate study areas and do not necessarily depict accepted national boundaries).

activities and fire disturbance by 2030 (1.3 Pg C, annual increase of 0.04 Pg C) and 2060 (2.5 Pg C, annual increase of 0.04 Pg C). Under existing policy scenarios, China's CO_2 emissions are projected to reach approximately 10.8 Gt in 2030 and 7.2 Gt in 2060, according to reports by the International Energy Agency (IEA, 2023) and the Ministry of Ecology and Environment of China (2021). Previous studies indicate terrestrial ecosystems could offset 13.6% of emissions by 2030 and 23% by 2060 (Huang et al., 2022), with forests accounting for 6.1% and 10.0% when considering future forest area change (Liu et al., 2024). The offset effect is 3% by 2030 and 4.4% by 2060 for existing forest without considering future area change (Huang et al., 2022; Liu et al., 2024). Our studies indicate the offset effect is 1.4% by 2030 and 2.0% by 2060 without considering future area change and growth of existing natural forest. Thus, FAFD can contribute 46.67% and 45.45% of total offset of existing forest by 2030 and 2060, respectively. While current forest sequestration capacity is insufficient to fully offset emissions, the future potential is great with broader and more intensive afforestation and reforestation actions, declining forest wood demand and proactive and effective fire prevention measures.

It is essential to plant high carbon-sequestration tree species to achieve China's carbon neutrality goal by 2060 (Qin et al., 2024; Xu et al., 2023). Our findings show significant differences in the net carbon sequestration capacities of tree species across regions (Fig. 9). Therefore, optimizing species selection, such as selecting tree species with strong carbon sequestration potential in newly established plantations and diversifying plantings, and ensuring continuous maintenance, can further enhance the national carbon sequestration capacity (Qin et al., 2024; Xu et al., 2023). In addition, expanding the planting of drought-tolerant species like *Populus* and desert tree species in regions with low-vegetation areas such as Inner Mongolia, southern Ningxia, and Xinjiang, is also an important strategy to enhance the national forest carbon sequestration.

Reduction of emissions from forest harvest and fire is also critical. Although harvested wood retains substantial carbon, it gradually releases carbon during processing, transport, and use. Therefore, improving the production process of forest products, enhancing wood

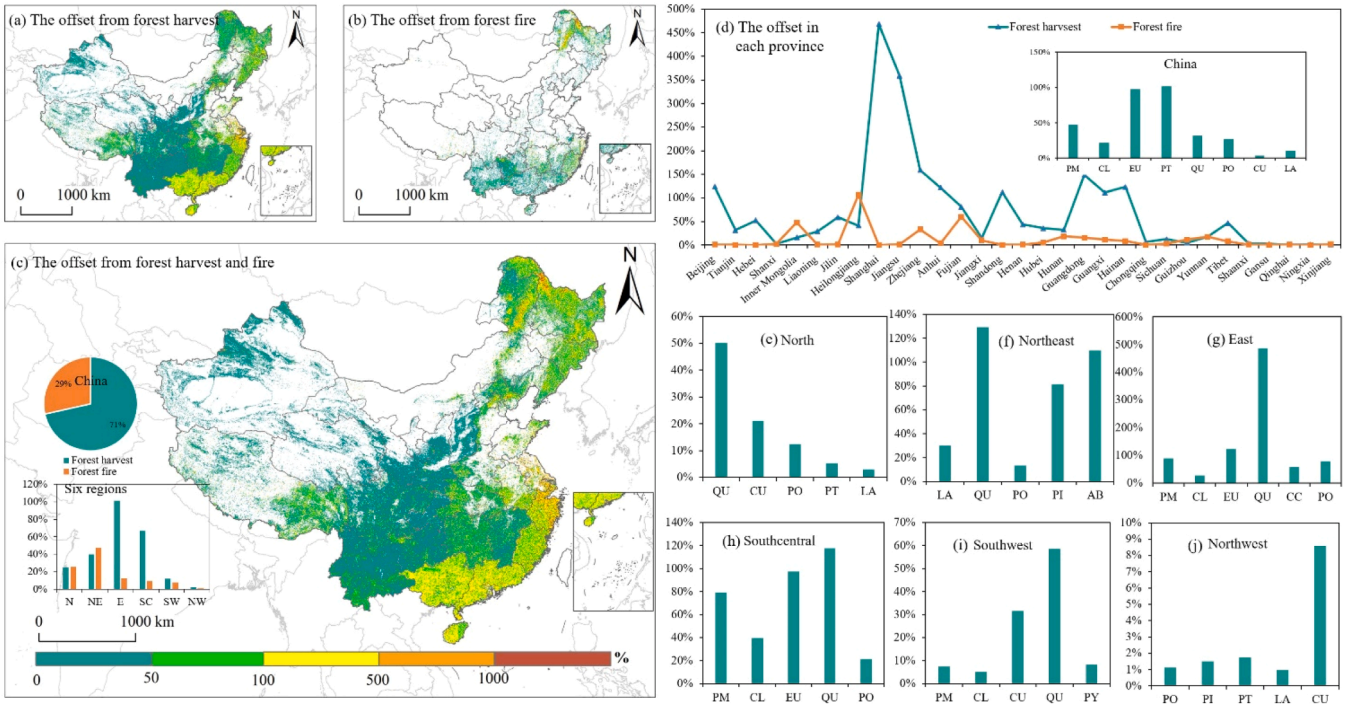

Fig. 9. Carbon emission offset from forest harvest and fire on the carbon sequestration from forestation (Note: map lines delineate study areas and do not necessarily depict accepted national boundaries).

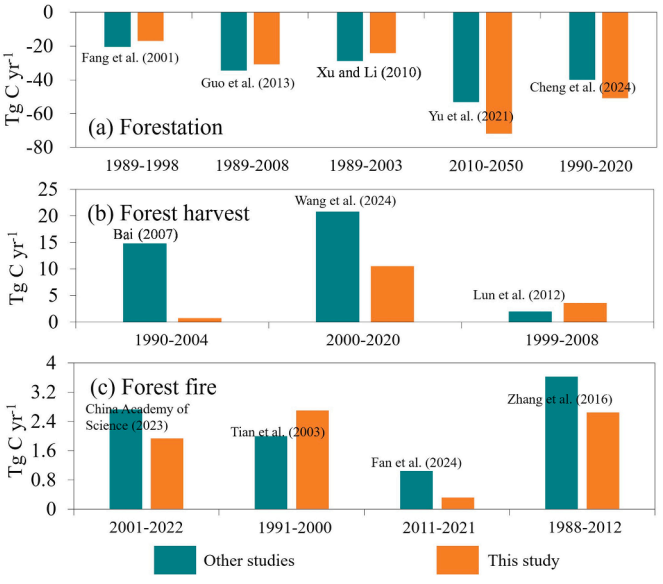

Fig. 10. Carbon budget comparison of forestation (a), forest harvest (b) and forest fire (c) with other studies.

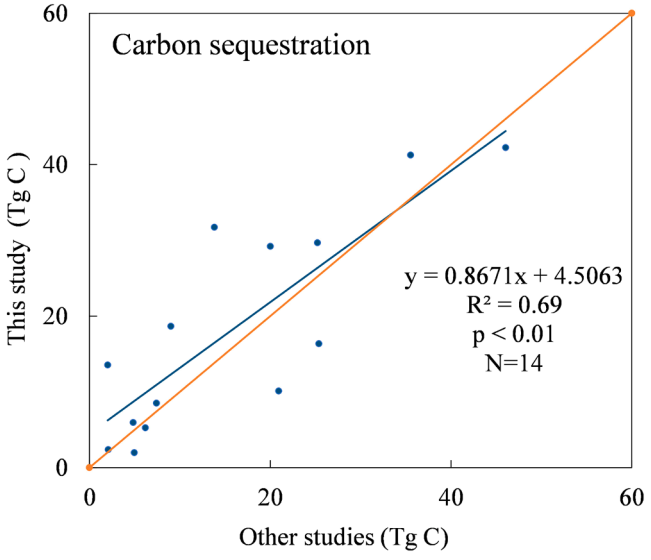

Fig. 11. Comparison of estimated carbon sequestration from forestation with previous inventory based studies at provincial scale.

utilization efficiency, and reducing waste are essential strategies. These goals can be achieved through the adoption of more efficient processing technologies and low-carbon transportation methods. Additionally, extending harvest cycles and wood product lifespan can also reduce carbon emissions. Fire emissions can be minimized through better monitoring, early warning systems, effective firefighting, and rational forest planning.

5. Conclusions

Forest activities and disturbances in China have led to significant shifts in forest carbon stocks, with forest harvest, forest fire, and forestation each contributing uniquely to these changes. This study reveals that harvest and fire notably impact the net carbon sequestration capacity of forests, with emissions from these activities offsetting 38.26% and 15.26% of the carbon sequestered by forestation, respectively—altogether offsetting nearly half of the gains from forestation efforts. Consequently, these activities present a net carbon sequestration of 710.64±136.4 Tg C across impacted areas. The offset effects exhibit considerable spatial variability, with most regions showing offsets below 50%. However, in eastern, southern, and southeastern China, carbon offsets from forest harvesting ranged from 50% to 500%, with areas in Jiangsu, Zhejiang, Fujian, Guangdong, and Guangxi exceeding 200%

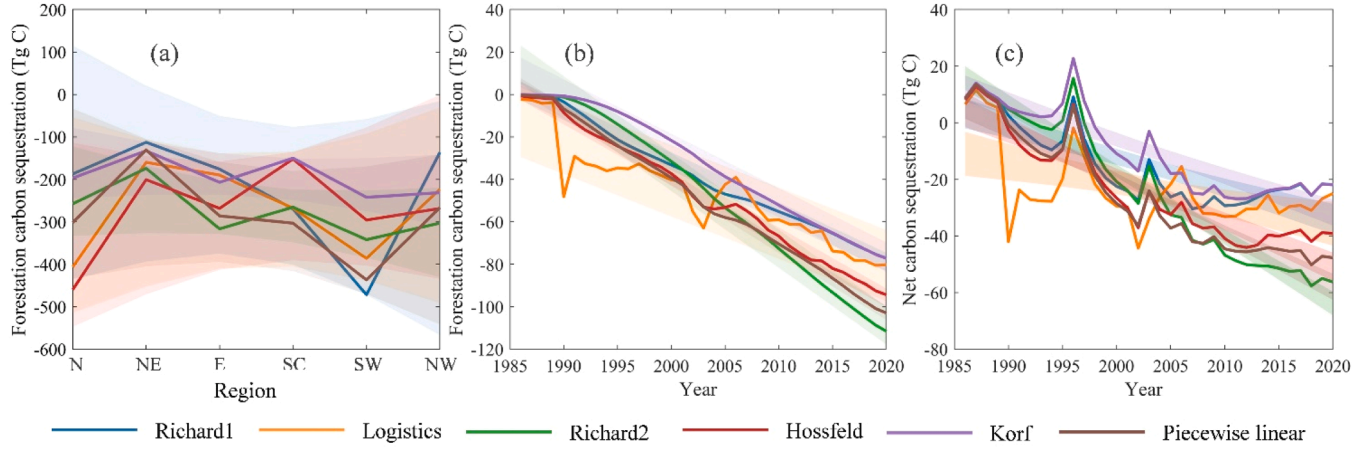

Fig. 12. Carbon sequestration from forestation in different regions (a) and the entire nation (b); and the total carbon budget from FAFD (c) under six growth curves. Note: Shaded sections represent 95% confidence intervals.

due to the high output from commercial plantations. In addition, fire in regions like the Greater Khingan Mountains contributed high offset levels. At a national scale, the offset impact from forest harvesting varies among tree species, spanning from 3.51% to 101.27%, with an average offset of 42.52%. These findings suggest that to optimize the carbon sequestration potential of forestation, carbon emissions from harvest and fire must be addressed. Future forest management initiatives should therefore be designed with careful consideration, especially in regions where carbon offsets from harvest and fire are substantial, as targeted management could significantly enhance carbon sequestration outcomes.

Data availability

The data were derived from the following resources available in the public domain: *China Forestry Statistical Yearbook*, URL: http://202.99.63.178/c/www/tjnj.jhtml; *National Bureau of Statistics of China*, URL: https://www.stats.gov.cn/; *Forestry Professional Knowledge Service System*, URL: http://lygc.lknet.ac.cn; *Forestry Industry of China*, URL: http://202.99.63.178/c/www/tjnj.jhtml; Land use/cover dataset (Zhang et al. (2024)), URL: https://data.casearth.cn/thematic/glc_fcs30/314; Forest fire dataset (Long et al. (2019)), URL: https://vapd.gitlab.io/post/gabam/; Forest disturbance dataset (Liu et al. (2023)), URL: https://github.com/liuzh811/DisturbMapping_China

CRediT authorship contribution statement

Jin Mai: Writing – original draft, Visualization, Validation, Software, Methodology, Investigation, Formal analysis, Conceptualization. **Yaoliang Chen:** Writing – review & editing, Writing – original draft, Supervision, Resources, Methodology, Investigation, Funding acquisition, Formal analysis, Conceptualization. **Qinghai Song:** Supervision, Methodology. **Zhiying Xu:** Supervision, Methodology. **Dengsheng Lu:** Supervision, Methodology, Funding acquisition. **Geping Luo:** Supervision, Methodology.

Declaration of competing interest

We declare that we have no financial and personal relationships with other people or organizations that can inappropriately influence our work, there is no professional or other personal interest of any nature or kind in any product, service and/or company that could be construed as influencing the position presented in, or the review of, the manuscript entitled.

Acknowledgments

This work was supported by the National Key Research and Development Program of China (2021YFD2200400102) and the National Natural Science Foundation of China (42277450). We are also grateful to all the data contributors who made this research possible.

Supplementary materials

Supplementary material associated with this article can be found, in the online version, at doi:10.1016/j.agrformet.2025.110830.

Data availability

Data will be made available on request.

References

Akagi, S.K., Yokelson, R.J., Wiedinmyer, C., Alvarado, M.J., Reid, J.S., Karl, T., Crounse, J.D., Wennberg, P.O., 2011. Emission factors for open and domestic biomass burning for use in atmospheric models. Atmos. Chem. Phys 11 (9), 4039–4072. https://doi.org/10.5194/acpd-10-27523-2010.

Allen, C.D., Macalady, A.K., Chenchouni, H., Bachelet, D., McDowell, N., Vennetier, M., Kitzberger, T., Rigling, A., Breshears, D.D., Hogg, E.H., Gonzalez, P., Fensham, R., Zhang, Z., Castro, J., Demidova, N., Lim, J.-H., Allard, G., Running, S.W., Semerci, A., Cobb, N., 2010. A global overview of drought and heat-induced tree mortality reveals emerging climate change risks for forests. For. Ecol. Manage 259 (4), 660–684. https://doi.org/10.1016/j.foreco.2009.09.001.

Anderegg, W.R., Schwalm, C., Biondi, F., Camarero, J.J., Koch, G., Litvak, M., Ogle, K., Shaw, J.D., Shevliakova, E., Williams, A.P., Wolf, A., Ziaco, E., Pacala, S., 2015. Forest ecology. Pervasive drought legacies in forest ecosystems and their implications for carbon cycle models. Science 349 (6247), 528–532. https://doi.org/10.1126/science.aab1833.

Bai, Y., 2007. Carbon Flow and Stock of Harvested Wood Products in China. China Academy of Forestry, Beijing.

Binte Shahid, S., Lacey, F.G., Wiedinmyer, C., Yokelson, R.J., Barsanti, K.C., 2024. Neivav1.0: Next-generation emissions inventory expansion of akagi et al. (2011) version 1.0. Geosci. Model. Dev 17 (21), 7679–7711. https://doi.org/10.5194/gmd-17-7679-2024.

Bougma, P.-t.C., Bondé, L., Yaro, V.S.O., Gebremichael, A.W., Ouédraogo, O., 2023. Assessing carbon emissions from biomass burning in croplands in burkina faso. west. afr. Fire 6 (10). https://doi.org/10.3390/fire6100402.

Bousquet, P., Peylin, P., Ciais, P., Le Quéré, C., Friedlingstein, P., Tans, P.P., 2000. Regional changes in carbon dioxide fluxes of land and oceans since 1980. Science 290 (5495), 1342–1346. https://doi.org/10.1126/science.290.5495.1342.

Chang, X., Xing, Y., Wang, J., Yang, H., Gong, W., 2022. Effects of land use and cover change (LUCC) on terrestrial carbon stocks in China between 2000 and 2018. Resour. Conserv. Recy 182. https://doi.org/10.1016/j.resconrec.2022.106333.

Chen, Y., Luo, G., Maisupova, B., Chen, X., Mukanov, B.M., Wu, M., Mambetov, B.T., Huang, J., Li, C., 2016. Carbon budget from forest land use and management in Central Asia during 1961–2010. Agric. For. Meteorol 221, 131–141. https://doi.org/10.1016/j.agrformet.2016.02.011.

Cheng, F., Tian, J., He, J., He, H., Liu, G., Zhang, Z., Zhou, L., 2023. The spatial and temporaldistribution of China's forest carbon. Front. Ecol. Evol 11, 4106. https://doi.org/10.3389/fevo.2023.1110594.
Cheng, K., Yang, H., Tao, S., Su, Y., Guan, H., Ren, Y., Hu, T., Li, W., Xu, G., Chen, M., Lu, X., Yang, Z., Tang, Y., Ma, K., Fang, J., Guo, Q., 2024. Carbon storage through China's planted forest expansion. Nat. Commun 15 (1), 4106. https://doi.org/10.1038/s41467-024-48546-0.
China Academy of Sciences., 2023. Blue book of carbon emissions from forest fire. Retrieved form https://iae.cas.cn/gb2019/xwzx_156509/ttxw_156510/202312/P020231212296936577850.pdf.
Dai, L., Jia, J., Yu, D., Lewis, B.J., Zhou, L., Zhou, W., Zhao, W., Jiang, L., 2013. Effects of climate change on biomass carbon sequestration in old-growth forest ecosystems on changbai mountain in northeast China. For. Ecol. Manage 300, 106–116. https://doi.org/10.1016/j.foreco.2012.06.046.
Deng, G., Lyu, M., Xiong, X., 2023. Understory ferns removal downregulates microbial carbon use efficiency and carbon accrual in previously degraded lands. Agric. For. Meteorol 340, 109631. https://doi.org/10.1016/j.agrformet.2023.109631.
Department of Climate Change, Ministry of Ecology and Environment of China., 2018. Third national communication on climate change of the people's republic of China. Retrieved from https://newsroom.unfccc.int/non-annex-I-NCs.
Department of Climate Change, National Development and Reform Commission of China., 2004. National development and reform commission of China. Initial national communication on climate change of the people's republic of China. Retrieved from https://newsroom.unfccc.int/non-annex-I-NCs.
Department of Climate Change, National Development and Reform Commission of China., 2012. Second national communication on climate change of the people's republic of China. Retrieved from https://newsroom.unfccc.int/non-annex-I-NCs.
Department of Climate Change, National Development and Reform Commission of China., 2016. First biennial update report on climate change of the people's republic of China. Retrieved from https://newsroom.unfccc.int/BURs.
Department of Climate Change, National Development and Reform Commission of China., 2018. Second biennial update report on climate change of the people's republic of China. Retrieved from https://newsroom.unfccc.int/non-annex-I-NCs.
Dixon, R.K., Solomon, A.M., Brown, S., Houghton, R.A., Trexier, M.C., Wisniewski, J., 1994. Carbon pools and flux of global forest ecosystems. Science 263 (5144), 185–190. https://doi.org/10.1126/science.263.5144.185.
Dobosz, B., Roman, K., Grzegorzewska, E., 2025. An estimation model of emissions from burning areas based on the tier method. Remote. Sens 17 (7). https://doi.org/10.3390/rs17071264.
Fan, D., Wang, M., Liang, T., He, H., Zeng, Y., Fu, B., 2024. Estimation and trend analysis of carbon emissions from forest fires in mainland China from 2011 to 2021. Ecol. Inf. 81. https://doi.org/10.1016/j.ecoinf.2024.102572.
Fang, J., Chen, A., Peng, C., Zhao, S., Ci, L., 2001. Changes in forest biomass carbon storage in China between 1949 and 1998. Science 292 (5525), 2320–2322. https://doi.org/10.1126/science.1058629.
Fang, J., Guo, Z., Piao, S., Chen, A., 2007. Estimation of terrestrial vegetation carbon sinks in China from 1981-2000. Sci. Chin. Earth. Sci 37 (6), 804–812.
Fang, J., Yu, G., Liu, L., Hu, S., Chapin, F.S., 2018. Climate change, human impacts, and carbon sequestration in China. P. Natl. Acad. Sci. USA 115 (16), 4015–4020. https://doi.org/10.1073/pnas.1700304115.
Fehrmann, L., Kleinn, C., 2006. General considerations about the use of allometric equations for biomass estimation on the example of Norway spruce in central Europe. For. Ecol. Manage 236 (2-3), 412–421. https://doi.org/10.1016/j.foreco.2006.09.026.
Friedlingstein, P., O'Sullivan, M., Jones, M.W., Andrew, R.M., Bakker, D.C.E., Hauck, J., Landschützer, P., Le Quéré, C., Luijkx, I.T., Peters, G.P., Peters, W., Pongratz, J., Schwingshackl, C., Sitch, S., Canadell, J.G., Ciais, P., Jackson, R.B., Alin, S.R., Anthoni, P., Barbero, L., Bates, N.R., Becker, M., Bellouin, N., Decharme, B., Bopp, L., Brasika, I.B.M., Cadule, P., Chamberlain, M.A., Chandra, N., Chau, T.-T.-T., Chevallier, F., Chini, L.P., Cronin, M., Dou, X., Enyo, K., Evans, W., Falk, S., Feely, R. A., Feng, L., Ford, D.J., Gasser, T., Ghattas, J., Gkritzalis, T., Grassi, G., Gregor, L., Gruber, N., Gürses, Ö., Harris, I., Hefner, M., Heinke, J., Houghton, R.A., Hurtt, G.C., Iida, Y., Ilyina, T., Jacobson, A.R., Jain, A., Jarníková, T., Jersild, A., Jiang, F., Jin, Z., Joos, F., Kato, E., Keeling, R.F., Kennedy, D., Klein Goldewijk, K., Knauer, J., Korsbakken, J.I., Körtzinger, A., Lan, X., Lefèvre, N., Li, H., Liu, J., Liu, Z., Ma, L., Marland, G., Mayot, N., McGuire, P.C., McKinley, G.A., Meyer, G., Morgan, E.J., Munro, D.R., Nakaoka, S.-I., Niwa, Y., O'Brien, K.M., Olsen, A., Omar, A.M., Ono, T., Paulsen, M., Pierrot, D., Pocock, K., Poulter, B., Powis, C.M., Rehder, G., Resplandy, L., Robertson, E., Rödenbeck, C., Rosan, T.M., Schwinger, J., Séférian, R., Smallman, T.L., Smith, S.M., Sospedra-Alfonso, R., Sun, Q., Sutton, A.J., Sweeney, C., Takao, S., Tans, P.P., Tian, H., Tilbrook, B., Tsujino, H., Tubiello, F., van der Werf, G. R., van Ooijen, E., Wanninkhof, R., Watanabe, M., Wimart-Rousseau, C., Yang, D., Yang, X., Yuan, W., Yue, X., Zaehle, S., Zeng, J., Zheng, B., 2023. Global carbon budget 2023. Earth. Syst. Sci. Data 15 (12), 5301–5369. https://doi.org/10.5194/essd-15-5301-2023.
Goward, S. N., C. Huang, F. Zhao, K. Schleeweis, K. Rishmawi, M. Lindsey, J.L. Dungan, and A. Michaelis. 2016. NACP NAFD Project: forest disturbance history from landsat, 1986-2010. https://doi.org/10.3334/ORNLDAAC/1290.
Guan, J., Du, s., Cheng, J., Wu, C., Li, G., Lei, D., Zhang, J., He, Q., Shi, W., 2016. Current stocks and rate of sequestration of forest carbon in Gansu Province. China. Chin. J. Plant. Ecol 40 (4), 304–317. https://doi.org/10.17521/cjpe.2016.0017.
Guimberteau, M., Ciais, P., Ducharne, A., Boisier, J.P., Dutra Aguiar, A.P., Biemans, H., De Deurwaerder, H., Galbraith, D., Kruijt, B., Langerwisch, F., Poveda, G., Rammig, A., Rodriguez, D.A., Tejada, G., Thonicke, K., Von Randow, C., Von Randow, R.C.S., Zhang, K., Verbeeck, H., 2017. Impacts of future deforestation and climate change on the hydrology of the amazon basin: A multi-model analysis with a new set of land-cover change scenarios. Hydrol. Earth. Syst. Sci 21 (3), 1455–1475. https://doi.org/10.5194/hess-21-1455-2017.
Guo, Z., Hu, H., Li, P., Li, N., Fang, J., 2013. Spatio-temporal changes in biomass carbon sinks in China's forests from 1977 to 2008. Sci. Chi. Life. Sci 56 (7), 661–671. https://doi.org/10.1007/s11427-013-4492-2.
Gurney, K.R., Law, R.M., Denning, A.S., Rayner, P.J., Baker, D., Bousquet, P., Bruhwiler, L., Chen, Y.H., Ciais, P., Fan, S., Fung, I.Y., Gloor, M., Heimann, M., Higuchi, K., John, J., Maki, T., Maksyutov, S., Masarie, K., Peylin, P., Prather, M., Pak, B.C., Randerson, J., Sarmiento, J., Taguchi, S., Takahashi, T., Yuen, C.W., 2002. Towards robust regional estimates of co2 sources and sinks using atmospheric transport models. Nature 415 (6872), 626–630. https://doi.org/10.1038/415626a.
Han, M., Liang, Y., 2015. Study on changes in forest biomass carbon storage based on forest inventory data in Guangxi. For. Resour. Manag 6, 111–122. https://doi.org/10.13466/j.cnki.lyzygl.2015.06.021.
Hansen, M.C., Potapov, P.V., Moore, R., Hancher, M., Turubanova, S.A., Tyukavina, A., Thau, D., Stehman, S.V., Goetz, S.J., Loveland, T.R., Kommareddy, A., Egorov, A., Chini, L., Justice, C.O., Townshend, J.R., 2013. High-resolution global maps of 21st-century forest cover change. Science 342 (6160), 850–853. https://doi.org/10.1126/science.1244693.
Harmon, M.E., Fasth, B.G., Yatskov, M., Kastendick, D., Rock, J., Woodall, C.W., 2020. Release of coarse woody detritus-related carbon: A synthesis across forest biomes. Carbon. Balance. Manag 15 (1), 1. https://doi.org/10.1186/s13021-019-0136-6.
He, H., Wang, S., Zhang, L., Wang, J., Ren, X., Zhou, L., Piao, S., Yan, H., Ju, W., Gu, F., Yu, S., Yang, Y., Wang, M., Niu, Z., Ge, R., Yan, H., Huang, M., Zhou, G., Bai, Y., Xie, Z., Tang, Z., Wu, B., Zhang, L., He, N., Wang, Q., Yu, G., 2019. Altered trends in carbon uptake in China's terrestrial ecosystems under the enhanced summer monsoon and warming hiatus. Natl. Sci. Rev 6 (3), 505–514. https://doi.org/10.1093/nsr/nwz021.
Houghton, R.A., 2005. Aboveground forest biomass and the global carbon balance. Glob. Change. Biol 11 (6), 945–958. https://doi.org/10.1111/j.1365-2486.2005.00955.x.
Houghton, R.A., Hackler, J.L., 2003. Sources and sinks of carbon from land-use change in China. Glob. Biogeochem. Cy 17 (2). https://doi.org/10.1029/2002gb001970.
Houghton, R.A., Hackler, J.L., Lawrence, K.T., 1999. The U.S. Carbon Budget: contributions from land-use change. Science 285 (5427), 574–578. https://doi.org/10.1126/science.285.5427.574.
Houghton, R.A., Hobbie, J.E., Melillo, J.M., Moore, B., Peterson, B.J., Shaver, G.R., Woodwell, G.M., 1983. Changes in the carbon content of terrestrial biota and soils between 1860 and 1980: a net release of CO_2 to the atmosphere. Ecol. Monogr 53 (3), 235–262. https://doi.org/10.2307/1942531.
Houghton, R.A., House, J.I., Pongratz, J., van der Werf, G.R., DeFries, R.S., Hansen, M.C., Le Quéré, C., Ramankutty, N., 2012. Carbon emissions from land use and land-cover change. Biogeosciences 9 (12), 5125–5142. https://doi.org/10.5194/bg-9-5125-2012.
Houghton, R.A., Nassikas, A.A., 2017. Global and regional fluxes of carbon from land use and land cover change 1850–2015. Glob. Biogeochem. Cy 31 (3), 456–472. https://doi.org/10.1002/2016gb005546.
Huang, Y., Sun, W., Qin, Z., Zhang, W., Yu, Y., Li, T., Zhang, Q., Wang, G., Yu, L., Wang, Y., Ding, F., Zhang, P., 2022. The role of China's terrestrial carbon sequestration 2010-2060 in offsetting energy-related CO_2 emissions. Natl. Sci. Rev 9 (8), nwac057. https://doi.org/10.1093/nsr/nwac057.
Huang, Z., Du, H., Li, X., Mao, F., 2023. A review of research on land use/cover change and its impact on forest carbon balance. Nat. Remote. Sens. Bull 0 (0), 1–21. https://doi.org/10.11834/jrs.20233169.
International Energy Agency, 2023. World energy outlook. Retrieved from https://origin.iea.org/reports/world-energy-outlook-2023.
IPCC, 2006. In: Eggleston, H.S., Buendia, L., Miwa, K., Ngara, T., Tanabe, K. (Eds.), 2006 IPCC guidelines for national greenhouse gas inventories. Prepared by the National Greenhouse Gas Inventories Programme. Institute for Global Environmental Strategies (IGES), Hayama, Japan.
IPCC, 2019. IPCC special report on Climate Change, Desertification, land degradation, Sustainable Land Management, Food Security, and greenhouse gas fluxes in terrestrial ecosystems. Retrieved from https://www.ipcc.ch/report/ar6/syr/downloads/report/IPCC_AR6_SYR_LongerReport.pdf.
Jia, S., 2014. Dynamic changes of carbon storage and estimation of carbon sink economic value of high-forest in Henan Province. J. Henan. Agric. Sci 43 (5), 149–153. https://doi.org/10.15933/j.cnki.1004-3268.2014.05.041.
Jiang, F., Chen, J.M., Zhou, L., Ju, W., Zhang, H., Machida, T., Ciais, P., Peters, W., Wang, H., Chen, B., Liu, L., Zhang, C., Matsueda, H., Sawa, Y., 2016. A comprehensive estimate of recent carbon sinks in China using both top-down and bottom-up approaches. Sci. Rep 6, 22130. https://doi.org/10.1038/srep22130.
Jiang, F., Wang, H.W., Chen, J.M., Zhou, L.X., Ju, W.M., Ding, A.J., Liu, L.X., Peters, W., 2013. Nested atmospheric inversion for the terrestrial carbon sources and sinks in China. Biogeosciences 10 (8), 5311–5324. https://doi.org/10.5194/bg-10-5311-2013.
Jiao, Y., Hu, H., 2005. Carbon storage and its dynamics of forest vegetation in Heilongjiang Province. Chin. J. Appl. Ecol 16 (12). https://doi.org/10.13287/j.1001-9332.2005.0329, 22448-2252.
Kaimowitz, D., 2018. Why forests? Why now? The science, economics and politics of tropical forests and climate change by frances seymour and jonah busch centre for global development, Washington, DC, 2016 Pp. 429 + xiv. ISBN 978 1 933286 85 3 Asia. Pac. Econ. Lit 32 (1), 148–149. https://doi.org/10.1111/apel.12226.
Kelly, L.T., Giljohann, K.M., Duane, A., Aquilue, N., Archibald, S., Batllori, E., Bennett, A. F., Buckland, S.T., Canelles, Q., Clarke, M.F., Fortin, M.J., Hermoso, V., Herrando, S., Keane, R.E., Lake, F.K., McCarthy, M.A., Moran-Ordonez, A., Parr, C.L., Pausas, J.G., Penman, T.D., Regos, A., Rumpff, L., Santos, J.L., Smith, A.L., Syphard, A.D.,

Tingley, M.W., Brotons, L., 2020. Fire and biodiversity in the anthropocene. Science 370 (6519). https://doi.org/10.1126/science.abb0355.
Kuemmerle, T., Olofsson, P., Chaskovskyy, O., Baumann, M., Ostapowicz, K., Woodcock, C.E., Houghton, R.A., Hostert, P., Keeton, W.S., Radeloff, V.C., 2011. Post-soviet farmland abandonment, forest recovery, and carbon sequestration in western ukraine. Glob. Change. Biol 17 (3), 1335–1349. https://doi.org/10.1111/j.1365-2486.2010.02333.x.
Li, B., 2015. Carbon storage dynamics of forest ecosystems, carbon sequestration potential of existing forest vegetation in Hunan Province. Central South University of Forestry and Technology, Changsha.
Li, L., 2012. Dynamic changes of forest vegetation carbon storage and carbon sink potential in Yunnan Province from 1992 to 2007. Yunnan University of Finance and Economics, Kunming.
Li, X., Wang, Y.-P., Lu, X., Yan, J., 2021. Diagnosing the impacts of climate extremes on the interannual variations of carbon fluxes of a subtropical evergreen mixed forest. Agr. For. Meteorol 307. https://doi/10.1016/j.agrformet.2021.108507.
Liu, B., 2015. Study on the characteristics of carbon storage of forest ecosystem in Shaanxi Province. Northwest A&F University, Xianyang.
Liu, J., Hu, J., Zhang, B., Zhou, X., Xiao, Q., Mei, H., 2017. Study on carbon storage and its distribution law of plantation vegetation in Hainan. Cent. South. For. Invent. Plan 36 (2), 52–54. https://doi.org/10.16166/j.cnki.cn43-1095.2017.02.012.
Liu, S., Wang, H., Li, H., Yu, Z., Luan, J., 2024. Projections of China's forest carbon storage and sequestration and ways of their potential capacity enhancement. Sci. Sil. Sin. 60 (4), 157–172. https://doi.org/10.11707/.1001-7488.LYKX20230206.
Liu, W., Guo, Z., Lu, F., Wang, X., Zhang, M., Liu, B., Wei, Y., Cui, L., Luo, Y., Zhang, L., Ouyang, Z., Yuan, Y., 2020. The influence of disturbance and conservation management on the greenhouse gas budgets of China's forests. J. Clean. Prod 261. https://doi.org/10.1016/j.jclepro.2020.121000.
Liu, Z., Wang, W.J., Ballantyne, A., He, H.S., Wang, X., Liu, S., Ciais, P., Wimberly, M.C., Piao, S., Yu, K., Yao, Q., Liang, Y., Wu, Z., Fang, Y., Chen, A., Xu, W., Zhu, J., 2023. Forest disturbance decreased in China from 1986 to 2020 despite regional variations. Commun. Earth. Env. 4 (1). https://doi.org/10.1038/s43247-023-00676-x.
Loboda, T. V., D. Chen, J.V. Hall, and J. He., 2018. Landsat-derived burn scar dNBR across Alaska and Canada, 1985-2015. https://doi.org/10.3334/ORNLDAAC/1564.
Long, T., Zhang, Z., He, G., Jiao, W., Tang, C., Wu, B., Zhang, X., Wang, G., Yin, R., 2019. 30 m resolution global annual burned area mapping based on landsat images and google earth engine. Remote. Sens 11 (5). https://doi.org/10.3390/rs11050489.
Lu, J., Feng, Z., Zhu, Y., 2019. Estimation of forest biomass and carbon storage in China based on forest resources inventory data. Forests 10 (8). https://doi.org/10.3390/f10080650.
Lun, F., Li, W., Liu, Y., 2012. Complete forest carbon cycle and budget in China, 1999–2008. For. Ecol. Manage 264, 81–89. https://doi.org/10.1016/j.foreco.2011.10.004.
Ma, Z., 2024. Characteristics of dynamic changes in forest carbon storage based on the 7th-9th forest resource inventory data in Ningxia. Shaanxi. For. Sci. Technol 52 (3), 40–45. https://doi.org/10.3969/j.issn.1001-2117.2024.03.007.
Ministry of Ecology and Environment of China., 2021. Transition to a carbon-neutral energy economy by 2060. Retrieved from https://www.mee.gov.cn/home/ztbd/2020/wfcsjssdgz/wfcsxwbd/ylgd/202104/P020210401595660592840.pdf.
National Forestry and Grassland Administration, 2018. Forestry Industry Standards of the China: regulations for age-class and age-group division of main tree-species. Retrieved from https://std.samr.gov.cn/hb/search/stdHBDetailed?id=8B1827F2424CBB19E05397BE0A0AB44A.
Olofsson, P., Woodcock, C. E., Baccini, A., Houghton, R. A., Ozdogan, M., Gancz, V., Blujdea, V., Torchinava, P., Tufekcioglu, A., Baskent, Z. A., 2009. The effects of land use change on terrestrial carbon dynamics in the black sea region. Regional aspects of climate-terrestrial-hydrologic interactions in non-boreal eastern europe, 175-181. https://doi.org/10.1007/978-90-481-2283-7_19.
Pan, Y., Birdsey, R.A., Fang, J., Houghton, R., Kauppi, P.E., Kurz, W.A., Phillips, O.L., Shvidenko, A., Lewis, S.L., Canadell, J.G., Ciais, P., Jackson, R.B., Pacala, S.W., McGuire, A.D., Piao, S., Rautiainen, A., Sitch, S., Hayes, D., 2011. A large and persistent carbon sink in the world's forests. Science 333 (6045), 988–993. https://doi.org/10.1126/science.1201609.
Pan, Y., Birdsey, R.A., Phillips, O.L., Houghton, R.A., Fang, J., Kauppi, P.E., Keith, H., Kurz, W.A., Ito, A., Lewis, S.L., Nabuurs, G.J., Shvidenko, A., Hashimoto, S., Lerink, B., Schepaschenko, D., Castanho, A., Murdiyarso, D., 2024. The enduring world forest carbon sink. Nature 631 (8021), 563–569. https://doi.org/10.1038/s41586-024-07602-x.
Peng, C., Ma, Z., Lei, X., Zhu, Q., Chen, H., Wang, W., Liu, S., Li, W., Fang, X., Zhou, X., 2011. A drought-induced pervasive increase in tree mortality across canada's boreal forests. Nat. Clim. Change 1 (9), 467–471. https://doi.org/10.1038/nclimate1293.
Peylin, P., Law, R.M., Gurney, K.R., Chevallier, F., Jacobson, A.R., Maki, T., Niwa, Y., Patra, P.K., Peters, W., Rayner, P.J., Rödenbeck, C., van der Laan-Luijkx, I.T., Zhang, X., 2013. Global atmospheric carbon budget: results from an ensemble of atmospheric CO_2 inversions. Biogeosciences 10 (10), 6699–6720. https://doi.org/10.5194/bg-10-6699-2013.
Piao, S., Fang, J., Ciais, P., Peylin, P., Huang, Y., Sitch, S., Wang, T., 2009. The carbon balance of terrestrial ecosystems in China. Nature 458 (7241), 1009–1013. https://doi.org/10.1038/nature07944.
Piao, S., He, Y., Wang, X., Chen, F., 2022. Estimation of China's terrestrial ecosystem carbon sink: methods, progress and prospects. Sci. Chin. Earth. Sci 65 (4), 641–651. https://doi.org/10.1007/s11430-021-9892-6.
Piao, S., Liu, Z., Wang, T., Peng, S., Ciais, P., Huang, M., Ahlstrom, A., Burkhart, J.F., Chevallier, F., Janssens, I.A., Jeong, S.-J., Lin, X., Mao, J., Miller, J., Mohammat, A., Myneni, R.B., Peñuelas, J., Shi, X., Stohl, A., Yao, Y., Zhu, Z., Tans, P.P., 2017. Weakening temperature control on the interannual variations of spring carbon uptake across northern lands. Nat. Clim. Change 7 (5), 359–363. https://doi.org/10.1038/nclimate3277.
Pienaar, L.V.T., K.J., 1973. The Chapman-Richards generalization of Von Bertalanffy's growth model for basal area growth and yield in even-aged stands. For. Sci 19 (1973). https://doi.org/10.1093/FORESTSCIENCE/19.1.2.
Qin, J., Liu, P., Martin, A.R., Wang, W., Lei, Y., Li, H., 2024. Forest carbon storage and sink estimates under different management scenarios in China from 2020 to 2100. Sci. Total. Env. 927, 172076. https://doi.org/10.1016/j.scitotenv.2024.172076.
Randerson. J.T. G.R. van der Werf L. Giglio, G.J. Collatz. P.S. Kasibhatla., 2018. Global fire emissions Database. Version 4.1(GFEDv4). https://doi.org/10.3334/ORNLDAAC/1293.
Saponaro, V., De Cáceres, M., Dalmonech, D., D'Andrea, E., Vangi, E., Collalti, A., 2025. Assessing the combined effects of forest management and climate change on carbon and water fluxes in european beech forests. For. Ecosyst 12. https://doi.org/10.1016/j.fecs.2024.100290.
Sitch, S., Huntingford, C., Gedney, N., Levy, P.E., Lomas, M., Piao, S.L., Betts, R., Ciais, P., Cox, P., Friedlingstein, P., Jones, C.D., Prentice, I.C., Woodward, F.I., 2008. Evaluation of the terrestrial carbon cycle, future plant geography and climate-carbon cycle feedbacks using five dynamic global vegetation models (dgvms). Glob. Change. Biol 14 (9), 2015–2039. https://doi.org/10.1111/j.1365-2486.2008.01626.x.
Spear, M.J., Hart, J., 2025. Modelling wood product service lives and residence times for biogenic carbon in harvested wood products: A review of half-lives, averages and population distributions. Forests 16 (7). https://doi.org/10.3390/f16071162.
Stephens, B.B., Gurney, K.R., Tans, P.P., Sweeney, C., Peters, W., Bruhwiler, L., Ciais, P., Ramonet, M., Bousquet, P., Nakazawa, T., Aoki, S., Machida, T., Inoue, G., Vinnichenko, N., Lloyd, J., Jordan, A., Heimann, M., Shibistova, O., Langenfelds, R. L., Steele, L.P., Francey, R.J., Denning, A.S., 2007. Weak northern and strong tropical land carbon uptake from vertical profiles of atmospheric co2. Science 316 (5832), 1732–1735. https://doi.org/10.1126/science.1137004.
Tang, Z., Xu, W., Zhou, G., Bai, Y., Li, J., Tang, X., Chen, D., Liu, Q., Ma, W., Xiong, G., He, H., He, N., Guo, Y., Guo, Q., Zhu, J., Han, W., Hu, H., Fang, J., Xie, Z., 2018. Patterns of plant carbon, nitrogen, and phosphorus concentration in relation to productivity in China's terrestrial ecosystems. Proc. Natl. Acad. Sci. USA 115 (16), 4033–4038. https://doi.org/10.1073/pnas.1700295114.
Tian, H., Xu, X., Lu, C., Liu, M., Ren, W., Chen, G., Melillo, J., Liu, J., 2011. Net exchanges of co2, ch4, and n2o between China's terrestrial ecosystems and the atmosphere and their contributions to global climate warming. J. Geophys. Res 116 (G2). https://doi.org/10.1029/2010jg001393.
Tian, X., Shu, L., Wang, M., 2003. Direct carbon emissions from chinese forest fires,1991-2000. Fire. Saf. Sci 12 (1), 6–10.
Tong, X., Brandt, M., Yue, Y., Ciais, P., Rudbeck Jepsen, M., Penuelas, J., Wigneron, J.P., Xiao, X., Song, X.P., Horion, S., Rasmussen, K., Saatchi, S., Fan, L., Wang, K., Zhang, B., Chen, Z., Wang, Y., Li, X., Fensholt, R., 2020. Forest management in southern China generates short term extensive carbon sequestration. Nat. Commun 11 (1), 129. https://doi.org/10.1038/s41467-019-13798-8.
Turner, M.G., 2010. Disturbance and landscape dynamics in a changing world. Ecology 91 (10), 2833–2849. https://doi.org/10.1890/10-0097.1.
van der Werf, G.R., Randerson, J.T., Giglio, L., Collatz, G.J., Mu, M., Kasibhatla, P.S., Morton, D.C., DeFries, R.S., Jin, Y., van Leeuwen, T.T., 2010. Global fire emissions and the contribution of deforestation, savanna, forest, agricultural, and peat fires (1997–2009). Atmos. Chem. Phys 10 (23), 11707–11735. https://doi.org/10.5194/acp-10-11707-2010.
van der Werf, G.R., Randerson, J.T., Giglio, L., van Leeuwen, T.T., Chen, Y., Rogers, B.M., Mu, M., van Marle, M.J.E., Morton, D.C., Collatz, G.J., Yokelson, R.J., Kasibhatla, P. S., 2017. Global fire emissions estimates during 1997–2016. Earth. Syst. Sci. Data 9 (2), 697–720. https://doi.org/10.5194/essd-9-697-2017.
Vicente-Serrano, S.M., Gouveia, C., Camarero, J.J., Begueria, S., Trigo, R., Lopez-Moreno, J.I., Azorin-Molina, C., Pasho, E., Lorenzo-Lacruz, J., Revuelto, J., Moran-Tejeda, E., Sanchez-Lorenzo, A., 2013. Response of vegetation to drought time-scales across global land biomes. Proc. Natl. Acad. Sci. USA 110 (1), 52–57. https://doi.org/10.1073/pnas.1207068110.
Von Gadow, K. H., G., 1998. Modeling Forest Development; Faculty of Forest and Woodland Ecology.
Wang, D., Ren, P., Xia, X., Fan, L., Qin, Z., Chen, X., Yuan, W., 2024. National forest carbon harvesting and allocation dataset for the period 2003 to 2018. Earth. Syst. Sci. Data 16 (5), 2465–2481. https://doi.org/10.5194/essd-16-2465-2024.
Wang, J., Feng, L., Palmer, P.I., Liu, Y., Fang, S., Bosch, H., O'Dell, C.W., Tang, X., Yang, D., Liu, L., Xia, C., 2020. Large chinese land carbon sink estimated from atmospheric carbon dioxide data. Nature 586 (7831), 720–723. https://doi.org/10.1038/s41586-020-2849-9.
Wang, N., 2014. Study on Distribution Patterns of Carbon Density and Carbon Stock in the Forest Ecosystem of Shanxi. Beijing Forestry University, Beijing.
Wang, Y., Cheng, Y., Gu, Z., Yang, J., Ren, H., 2022. Emission factors and inventories of carbonaceous aerosols from residential biomass burning in Guizhou Province. China. Atmos. 13 (10). https://doi.org/10.3390/atmos13101595.
Wang, Y., Li, C., Ochege, F.U., Han, Q., Hellwich, O., Wu, S., Luo, G., 2022. Contribution of cropland expansion to regional carbon stocks in an arid area of China: a case study in Xinjiang. Carbon. Manag 13 (1), 42–54. https://doi.org/10.1080/17583004.2022.2043446.
Wu, G., Tang, X., Ruan, H., Luo, X., 2019. Carbon storage and carbon sequestration potential based on forest inventory data in Jiangxi Province, China. J. Nanjing. For. Univ. (Nat. Sci. Ed.) 43 (1), 105–110. https://doi.org/10.3969/i.ssn.1000-2006.201711051.
Wu, Q., Ni, X., Sun, X., Chen, Z., Hong, S., Berg, B., Zheng, M., Chen, J., Zhu, J., Ai, L., Zhang, Y., Wu, F., 2025. Substrate and climate determine terrestrial litter

decomposition. Proc. .Natl. Acad. Sci. USA 122 (7), e2420664122. https://doi.org/10.1073/pnas.2420664122.
Xia X, X. J., Yuan W., 2023. Reconstructing long-term forest cover in China by fusing national forest inventory and 20 land use and land cover data sets. https://doi.org/10.12199/nesdc.ecodb.rs.2023.015.
Xu, B., Guo, Z., Piao, S., Fang, J., 2010. Biomass carbon stocks in China's forests between 2000 and 2050: a prediction based on forest biomass-age relationships. Sci. Chin. Life. Sci 53 (7), 776–783. https://doi.org/10.1007/s11427-010-4030-4.
Xu, H., Yue, C., Zhang, Y., Liu, D., Piao, S., 2023. Forestation at the right time with the right species can generate persistent carbon benefits in China. P. Natl. Acad. Sci. USA 120 (41), e2304988120. https://doi.org/10.1073/pnas.2304988120.
Xu, L., Wen, D., Zhu, J., He, N., 2017. Regional variation in carbon sequestration potential of forest ecosystems in China. Chin. Geogr. Sci 27 (3), 337–350.
Xu, X.L., Li, K.R., 2010. Biomass carbon sequestration by planted forests in China. Chin. Geogr. Sci 20 (4), 289–297. https://doi.org/10.1007/s11769-010-0401-9.
Yang, D., Zhang, H., Liu, Y., Chen, B., Cai, Z., Lü, D., 2017. Monitoring carbon dioxide from space: retrieval algorithm and flux inversion based on GOSAT data and using CarbonTracker-China. Adv. Atmos. Sci 34 (8), 965–976. https://doi.org/10.1007/s00376-017-6221-4.
Yang, J., Huang, X., 2021. The 30 m annual land cover dataset and its dynamics in China from 1990 to 2019. Earth. Syst. Sci. Data 13 (8), 3907–3925. https://doi.org/10.5194/essd-13-3907-2021.
Yang, L., Lin, Y., Kong, J., Yu, Y., He, Q., Su, Y., Li, J., Qiu, Q., 2023. Effects of fertilization and dry-season irrigation on the timber production and carbon storage in subtropical eucalyptus plantations. Ind. Crops. Prod 192. https://doi.org/10.1016/j.indcrop.2022.116143.
Yu, Z., Ciais, P., Piao, S., Houghton, R.A., Lu, C., Tian, H., Agathokleous, E., Kattel, G.R., Sitch, S., Goll, D., Yue, X., Walker, A., Friedlingstein, P., Jain, A.K., Liu, S., Zhou, G., 2022. Forest expansion dominates China's land carbon sink since 1980. Nat. Commun 13 (1), 5374. https://doi.org/10.1038/s41467-022-32961-2.
Yu, Z., Liu, S., Li, H., Liang, J., Liu, W., Piao, S., Tian, H., Zhou, G., Lu, C., You, W., Sun, P., Dong, Y., Sitch, S., Agathokleous, E., 2024. Maximizing carbon sequestration potential in chinese forests through optimal management. Nat. Commun 15 (1), 3154. https://doi.org/10.1038/s41467-024-47143-5.
Yu, Z., Zhou, G., Liu, S., Agathokleous, E., 2020. Impacts of forest management intensity on carbon accumulation of China's forest plantations. For. Ecol. Manage 472 (118252). https://doi.org/10.1016/j.foreco.2020.118252.
Zeide, B., 1989. Accuracy of equations describing diameter growth. Can. J. For. Res 19 (10), 1283–1286. https://doi.org/10.1139/x89-195.
Zeide, B., 1993. Analysis of growth equations. For. Sci 39 (3), 594–616. https://doi.org/10.1093/forestscience/39.3.594.
Zhang, C., Ju, W., Wang, D., Wang, X., Wang, X., 2018. Biomass carbon stocks and economic value dynamics of forests in Shandong Province from 2004 to 2013. Acta. Ecol. Sin 38 (5), 1739–1749. https://doi.org/10.5846/stxb201703280535.
Zhang, H.F., Chen, B.Z., van der Laan-Luijkx, I.T., Chen, J., Xu, G., Yan, J.W., Zhou, L.X., Fukuyama, Y., Tans, P.P., Peters, W., 2014. Net terrestrial co2exchange over China during 2001-2010 estimated with an ensemble data assimilation system for atmospheric CO_2. J. Geophys. Res.:. Atmos 119 (6), 3500–3515. https://doi.org/10.1002/2013jd021297.
Zhang, L., Lu, M., Ma, X., Zhang, X., 2025. Analysis and potential prediction of forest carbon sequestration and its economic value in Liaoning Province. Nat. Sci 13 (1), 31–41. https://doi.org/10.12677/ojns.2025.131004.
Zhang, P., 2009. Study on forest carbon stock in Beijing of China. Beijing Forestry University, Beijing.
Zhang, X., Zhao, T., Xu, H., Liu, W., Wang, J., Chen, X., Liu, L., 2024. GLC_FCS30D: the first global 30 m land-cover dynamics monitoring product with a fine classification system for the period from 1985 to 2022 generated using dense-time-series Landsat imagery and the continuous change-detection method. Earth. Syst. Sci. Data 16 (3), 1353–1381. https://doi.org/10.5194/essd-16-1353-2024.
Zhang, Y., Qin, D., Yuan, W., Jia, B., 2016. Historical trends of forest fires and carbon emissions in China from 1988 to 2012. J. Geophys. Res.:. Biogeosciences 121 (9), 2506–2517. https://doi.org/10.1002/2016jg003570.
Zheng, B., Ciais, P., Chevallier, F., Chuvieco, E., Chen, Y., Yang, H., 2021. Increasing forest fire emissions despite the decline in global burned area. Sci. Adv 7 (39), eabh2646. https://doi.org/10.1126/sciadv.abh2646.
Zhou, X., Dong, K., Tang, Y., Huang, H., Peng, G., Wang, D., 2023. Research progress on the decomposition process of plant litter in wetlands: A review. Water. (Basel) 15 (18). https://doi.org/10.3390/w15183246.